SKIN ERYTHEMA ASSESSMENT TECHNIQUES: REVIEW ARTICLE

Ramy Abdlaty[1], Qiyin Fang[1, 2*]

1: *School of Biomedical Engineering, McMaster University,*

2: *Engineering Physics, McMaster University,*

1280 Main street West, Hamilton, Ontario, L8S 4K1

Abstract

Erythema is superficial redness of the skin. Skin erythema may present due to many causes. One of the common causes is prolonged exposure to sun rays. Other than sun exposure, skin erythema is an accompanying sign of dermatological disease such as psoriasis and acne. Quantifying skin erythema, in patients, enables the dermatologist to assess the patient's skin health. Therefore, quantitative assessment of skin erythema was the target of several studies. The clinical standard for erythema evaluation is visual assessment. However, the former standard has some imperfections. For instance, it is subjective, and unqualified for precise color information exchange. To overcome these shortcomings, the past three decades witnessed various studies that aimed to achieve erythema objective assessment, such as diffuse reflectance spectroscopy (DRS), optical/ non-optical imaging methodologies, and electrical measurement techniques. This current review article revises various studies in the past three decades and discusses their methodologies, mathematical tactics for computation, and their limitations. In conclusion, the limitations of the earlier erythema assessment techniques are motivation for developing novel techniques.

Keywords: Skin, Erythema, cutaneous diseases, akin inflammation

1 Skin Erythema

Skin erythema, or flare, is the reddening reaction of the skin as a result of an external stimulus [1], immunological reaction with/out hypersensitivity to an allergen [2], or viral infection [3]. The flare size depends on multiple parameters, for instance, the distribution of the neural fibers and vascularization of the stimulated region. Likewise, the strength and the nature of the stimulus are factors that influence the peak size of the flare. Typically, the flair's peak intensity is reached shortly after the stimulus onset. In some cases, the flare is a result of an accumulative process, such as radiotherapy treatment for cancer.

Bruce and Lewis interpreted the flare reaction to be an axon reflex [4], [5]. Simply put, if a pernicious provocation occurred to the human skin's afferent nerve, it would alert skin fibers. The fibers, in turn, would respond to the alert by generating action potentials mainly to the spinal cord, where they are distributed to complementary axons. This leads to the dispensation of neuropeptides like P /calcitonin gene-related peptide (CGRP). The neuropeptides trigger vasodilation, increasing blood to the skin, and thereby creating a red appearance [1]. In a second interpretation, erythema is the output of an inflammatory cutaneous reaction associated with diseases such as acne, psoriasis, melasma, as well as fever. In severe skin reactions, skin erythema turns to superficial blistering [6]–[8]. The blisters are associated with wet desquamation that may take place due to exposure to certain bands of electromagnetic waves (EMW).

EMW, be it ultraviolet (UV), visible (VIS), or infrared (IR) waves, are external stimulus of erythema. Each of the mentioned spectral bands has an exposure threshold or 'minimal erythema dose' (MED) [9]; if reached, skin erythema is directly induced [10]. An intriguing example of MED is the transient flush erythema which takes place rapidly in people with fair skin, in the summer upon exposure to sunlight [10]. In addition to EMW exposure, physical pressure [11], skin ulceration [12], [13], application of cosmetic/medical topical agents, and electrical stimulation [14]–[17] are all external stimuli of skin erythema. Over and above, burns induce erythema around resultant scars [18].

Radiation dermatitis [19]–[23] is typically an equivalent term to radiotherapy-induced erythema. In this case, erythema is a cancer radiotherapy treatment linked side effect. The dermatitis reaction is interpreted as a skin response to damage to basal cells present in the epidermal layer. To ameliorate the damaged region, deeper skin layers proliferate to replace the impaired, superficial [24]. The radiation dermatitis MED trigger is inconstant. However, there

are patients' parameters, including skin type, age, and tumor specifications, that affect dermatitis conduction [25]. Despite the lack of knowledge on dose-intensity, there is a rough threshold dose for triggering skin erythema, above which causes skin reactions [25]. It is of interest determine if permanent skin color change occur in the case of intensity-modulated radiation therapy (IMRT) due to the reduction of the melanocytes in the irradiated region [24],[22],[25],[29]. Dermatitis does not only indicate underlying disease and compromises the patient's physical appearance, but also acts as an early warning sensor for possible treatment pause [27]. Based on prior facts, it becomes obvious that radiation dermatitis calls for systematic monitoring and quantitative assessment.

The purpose of this paper is to to review the techniques utilized by earlier studies of skin erythema assessment. The review is expected to produce a solid background and foundation for developing innovative approaches to quantitative and objective skin erythema assessment.

2 Assessment Techniques

A major goal for any skin erythema assessment technique is to objectively quantify the redness without the need for a skin biopsy or direct contact. A potential approach is a contacless technique that generates a real time graded redness intensity map. Moreover, it is anticipated that the erythema assessment standard device is miniaturized, easy to operate, and costeffective. This section reviews the techniques that were employed within the last three decades , to evaluate, grade or detect skin erythema. The review begins with visual assessment (VA) since it is the gold standard for skin erythema evaluation. Next to VA, common optical modalities used for skin erythema assessment are introduced. Other, less common erythema assessment techniques are highlighted in section 2.3. Alongside erythema assessment methodologies, various tactics of computing the erythema index are overviewed.

2.1 Visual Assessment (VA)

VA is the original [28] and the simplest technique for skin erythema assessment. VA's simplicity is a result of its tool/ equipment-independent nature. VA depends solely on an experienced radiotherapist to grade the intensities of skin erythema [29] based on a predetermined ordinal scale of grades. Erythema ordinal scales vary in the resolution between the minimum and the maximum redness intensities. For example, there are three [29] , four [30], [31], and ten [28] steps erythema scales used in the literature. One exemplary model, of the erythema scales, is shown in Table 1 [28]. Although these scales are convenient for rapid assessment, they lack linear transitions between equidistant steps and thus they may miss or exaggerate with distinct skin erythema intensities [32]. In addition to the nonlinearity of erythema ordinal scales, VA suffers from subjectivity, intra-observer variability dependence, and incapability of precise color communication. Despite all of VA's disadvantaged, it is still widely used compared to more objective, engineered solutions. VA is (1) preferred because it is fast, allowing for more patients to be seen in short period of time; (2) simple to use, as there is no need for operating/ adjusting any equipment; and (3) suitable to the fast-paced clinical environment, since the clinician can move easily between rooms [33].

Table 1: Example of an ordinal grading scale used for skin erythema visual assessment divided into 10 different qualitative reactions [28]

Grade	Erythematous reaction
0	No reaction
1	Marginal reaction
2	Slight perceptible erythema
3	A greater than slight reaction which is not sufficient to be classed as distinct
4	Distinct erythema
5	A greater than distinct reaction which is insufficient to be classed as well developed
6	Well developed, possibly spreading erythema
7	A greater reaction which is not sufficient to be classed as strong
8	Strong, deep erythema which may extend beyond the treatment site
9	A more intense reaction than above

2.2 Colorimetry Assessment (CA)

Regarding human skin, color is a critical and informative descriptor for both clinical and research purposes [34]–[37]. However, the acquisition and communication of color information visually are limited by the time dependency, the describing language, and the means of communication. For instance, although the human eye is capable of distinguishing between an enormous range of similar colors [38], linguistic description is unable to satisfactorily convey distinct color tones. The lack of color descriptors to communicate various tissue color tones in a quantitative manner motivated the development of engineered colorimetry tools/ instruments to detect, analyze and archive distinct skin color changes.

Color standards are well-known tools used to assess the progression of some skin diseases associated with skin color change. One of the earliest standards used for this purpose was a set of red colored papers with graded red intensities. A direct application of the red

papers set to the skin was used to demarcate the skin erythema induced by UV exposure. The use of the colored papers enabled the generation of UV dose–response curves [39]. The red set of papers were neither durable, nor reliable; since it is easily worn and hard to be typically reproduced. To overcome the shortcomings of red papers, reliable and longer lasting red photographic filters were developed as the alternative. Unfortunately, neither red papers nor photographic filters were sufficiently robust to quantitatively grade skin erythema. Consequently, both standards rapidly went out of use. As a result, research interest transitioned to developing novel, reliable, and inexpensive color scales.

Toward a convenient color scale, Taylor hyperpigmentation scale (THS) was developed. THS is based on an extensive statistical study of different skin colors. The study employed a great number of people of different racial backgrounds to obtain the maximal skin color divergence [33]. Consequently, THS developed 15 skin hue representative cards. Each card is divided into ten graded pigmented steps. As such, THS has a total of 150 different colors that are expected to represent all skin types at a confidence of 95% [33], [40]. Meanwhile, a Japanese group developed a new color tone scale based on Munsell color system [41]. The Japanese color tone was printed on flexible plastic bars. Each bar is divided into ten color tones. The entire set of bars was used in a clinical study to assess the laser treatment of solar lentigo [42]. The study was performed over approximately one year and recruited 81 Japanese female patients [42]. Skin color tone matching, by the aforementioned color scales, was achieved in two steps as shown in Figure 1**Error! Reference source not found.**. The first step was identifying the best hue that corresponds to the participant's skin color. The second step was scanning the identified hue-card to find the best matching hyperpigmented tone of the subject's skin as shown in Figure 1 [42].

The advantage of the color scales is the simplicity of operation and the potential quantification of skin color change which, in turn, facilitates easy data communication and archiving. Although color scales, or color-order systems [43] expanded the spectrum of describable colors, it is still far from being objective and vision acuity-independent. Once again, color scales are susceptible to wear and tear, which renders the color tones less discernible. Hence, there was a need to depend on instrumental solutions to function as robust colorimeters, in order to overcome subjectivity and attain more reliable outcomes.

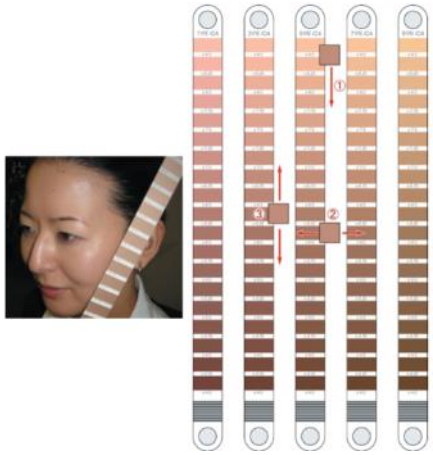

Figure 1: The process of allocating a color tone for human face commences with finding the closest possible match through the following steps, (1), a rough estimate is primarily determined by the operator and then (2) more precise pigmentation color is selected within left, right move, (3) followed by up and down adjustments. [42]

In order to overcome the limitations of color charts, systemic colorimeter devices were in demand. The colorimeter device function is to identify the tissue's apparent color using a 3-dimensional color space. The most common color space is the standard Commission Internationale de l'Eclairage (CIELab), which is represented by three axes: L*, a*, and b* [44]. The first axis is the gray-scale, symbolized by L*. The gray axis is divided into 100 divisions; starting from 0, (complete darkness), and ending at 100 (bright white). The second axis in CIELab space is the red-green axis, symboledized by a*. a*-axis has the red intensity on the positive side and the green intensity on the negative side. The third axis is the yellow-blue axis, symbolized by b*. b*-axis has the yellow intensity on the positive side and the blue intensity on the negative side. Both a* and b* axes are, in principle, applications of Hering's opponent color theory [45], which explains the human vision sensistivity to color detection. In the CIELab color space, the hue angle h^o is defined as the relevant psychometric of the visually perceived property of hue such as red, green, and magenta, and it is calculated using equation (1). It is prudent to know that the perceived color is not pure hue but is influenced by the color saturation as well. The color saturation is expressed by the displacement on the L* axis and termed chroma C, in the CIE. Chroma is calculated by equation (2) .

$$h^o = \arctan(\frac{b^*}{a^*}) \quad \textbf{(1)}$$

$$C = \sqrt{(a^*)^2 + (b^*)^2} \quad \textbf{(2)}$$

Color detection accuracy, in CIELab, is dependent on three factors, 1) the illuminating light specifications, 2) the light modulation by the tissue under test, and 3) the human vision attributes. CIELab strictly delineates these factors. First, the CIELab specifies the standard illumination for color measurements as published in tabulated formats [44], [46], [47]. Second, CIELab identifies the standard for the spectrometer applied to measure the light modulation in the range of the VIS region [46]. Third, the human visual system was investigated and the three matching color functions: $\bar{\mathbf{x}}$, $\bar{\mathbf{y}}$, and $\bar{\mathbf{z}}$ were determined. There are three matching colour functions because human vision interprets color using a trichromatic system [47]–[49]. The CIELab color system is a convenient, robust way for communicating color information; moreover, it is able to measure the differences between the perceived tissue colors. The difference (ΔE) between two colors is represented by the square root of the displacement of both colors in L*a*b* coordinates as shown in equation (3) [44].

$$\Delta E = [(\Delta L^*)^2 + (\Delta a^*)^2 + (\Delta b^*)^2]^{1/2} \quad \textbf{(3)}$$

2.3 Spectra-based Assessment

Spectral reflectance concept has been involved in the objective assessment of the skin color for a long time [40]. This concept has contributed in developing robust and reliable instruments such as the tristimulus instruments and the narrow-band spectrometers. The tristimulus instruments, such as Minolta chromameter, depends mainly on the measurement of the reflected light within three central wavelengths. Narrow-band spectrometers, unlike tristimulus instruments, such as the Dermaspectrometer, erythema meter, and Mexameter, measure the reflected light in specific-bands, mainly the red and green ones.

Tristimulus Colorimetry instruments were originally developed to objectively and reliably measure color information akin to the human visual system. Simply, the method of measurement depends on illuminating the tissue under investigation with a polychromatic light source and detecting the back-reflected intensity through three separate spectral channels. One or two-dimensional array of photodiodes are used for light detection. Minolta chromameter is a common example of the tristimulus colorimeters [18], [50]–[55]. Minolta instrument illuminates the object using a xenon light source and collects the diffusely back-reflected intensity at three central wavelength bands: 450, 560, and 600 nm. The instrument uses a mapping transformation to a color space such as CIELab standard in order to elucidate the object color. Minolta chromameter gains a good reputation due to its robustness and replicability [53]. Based on this reputation, Minolta chromameter color data was examined in comparison to visual grading for investigating skin blanching onset in response to the application of a topical corticosteroid agent on volunteers for three subsequent days [51]. The results of the study verified the higher performance of Minolta chromameter in distinguishing the blanching effect as shown in Figure 2. The study, also, prooved that the L* axis value is the most sensitive component in the color space for discriminating the skin blanching.

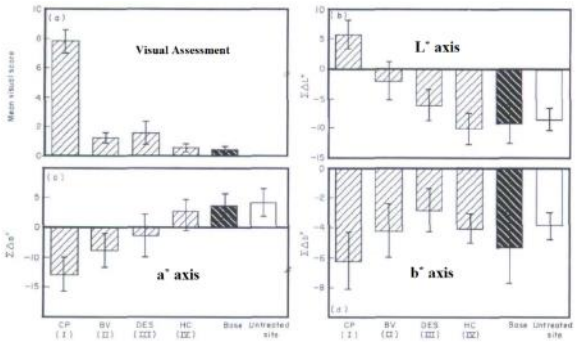

Figure 2: (a) Algebraic sum (mean ± std) for the visual assessment score, (b) the gray scale values $\sum \Delta \boldsymbol{L}^*$, (c) the red-green values $\sum \Delta \boldsymbol{a}^*$, and (d) the yellow-blue values $\sum \Delta \boldsymbol{b}^*$ for the skin color change induced by applying a topical corticosteroid agent using the Minolta Chromameter. [51]

The chromameter is inexpensive way for objectively measuring skin color. However, the shortcoming of such way is the necessity for systemic calibration each time they are used. Hence, an overhead time is spent to set up the instrument for operation. Therefore, it became inappropriate to use chromameter in the daily clinical practice.

Narrowband Spectroscopic Devices' principle of operation is based on the fact that the green and red portions of the visible spectra suffice to estimate the change in skin's pigmentations: hemoglobin, and melanin, in a quantitative approach [56]–[60]. For instance, the skin redness/ erythema severity is quantitatively estimated by subtracting the melanin effect from the green filter absorbance [56]. Other studies quantitatively evaluated erythema by only computing the changes in the hemoglobin content and negligibly consider the melanin's effect [61], [62].

As a direct application, a study reported the development of a portable device called the erythema meter [63], [64]. The device measures the skin's back-

reflected light within the red and the green spectral bands. The measured back reflected light gives the input to roughly estimate the cutaneous hemoglobin content. The hemoglobin content estimation is based on calculating the erythema index (EI), as displayed in equation (4).

$$EI = \log_{10}\left(\frac{Ref.red\ \ light\ int.}{Ref.Green\ \ light\ int.}\right) \quad (4)$$

In conjunction with the erythema meter, two more instruments are common in the class of the narrow band devices: the Dermaspectrometer [56], and the Mexameter [65]. The Dermaspectrometer device integrates two light-emitting diodes (LED) to illuminate the targeted skin ROI [56]. One LED emits at 568 nm (green band) and the other emits at 655 nm (red band). The skin's reflected intensities at the two wavelengths are detected and analyzed to provide both the melanin and the erythema indices.

The Mexameter, unlike the Dermaspectrometer, uses 16 integrated LED sources combined in one probe emitting at three separate bands; green (568 nm), red (660 nm), and near-infrared (NIR) (880 nm) bands. The Mexameter computes the skin's melanin index (MI) based on the measured red and NIR back reflected light as demonstrated in equation **Error! Reference source not found.**). The erythema index is computed based on the measured back reflected light in the green and red bands as demonstrated equation **Error! Reference source not found.**) [60], [66]. A sample type of the Mexameter is shown in Figure 3.

$$MI = \frac{500}{\log 5 * [\log(NIR_{refl}/Red_{refl}) + \log 5]} \quad (5)$$

$$EI = \frac{500}{\log 5 * [\log(Red_{refl}/Green_{refl}) + \log 5]} \quad (6)$$

The Mexameter is more sophisticated and expensive in contrast with the Dermaspectrometer. In terms of advantages, it has an accuracy range of ± 5% provided that three readings are obtained [65]. As a result, it is commonly used in cosmetic and pharmaceutical cutaneous research studies. Recently, it was approved to be put to use in: skin melasma investigation [65], skin toxicity diagnosis, and in monitoring melanin content variation due to radiotherapy [67].

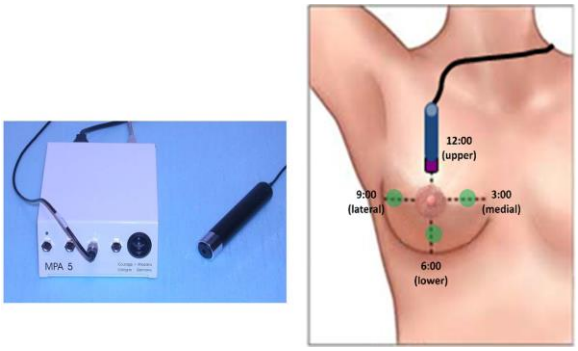

Figure 3: (a) the Mexameter device is equipped with a circular probe of 5 mm diameter and 20 mm2 surface area. (b) Example of using the Mexameter to quantitatively assess the skin damage attributable to breast cancer radiotherapy treatment [67].

The narrow-band spectroscopy principle is an active approach for objective assessment of skin erythema. Thus, it has been used in a real-time measurement for an artificial induced skin erythema study [11]. The study used an RGB sensor to measure the skin erythema due to an instantenous applied pressure, and monitor the temporal evolution of erythema in case of a constant pressure. In sum, the narrow-band devices are able to provide successful figures for the two skin pigmentation indices: the erythema and the melanin. However, they lack the potential for fully interpreting the skin color changes. Hence, the measurement of the skin's total diffuse reflectance was a more appropriate approach to perform this interpretation.

Diffuse reflectance spectroscopy (DRS) systems are involved in the measurement of the total diffusely back-reflected polychromatic light out of an illuminated object. Regarding human skin, the total diffusely reflected light is the summation of the back-reflected light excluding the specular reflected light. The excluded portion of the reflected light accounts for only 4:7 % of the total reflected light [68]. However, it probes the skin surface information including the refractive index. Conversely, the diffusely back-reflected light checks out the structures beneath the tissue surface, such as the underlying vascularization and pigments, by scattering inside the tissue before bouncing back. DRS measurements can be accomplished using both time domain- [69], [70], and frequency domain- [71], [72] based techniques.

DRS has been used in investigating divergent skin signs associated with cutaneous diseases [21], [73]–[75]. DRS systems were implemented utilizing multiple optical configurations including the integrating sphere (IS)-based DRS [76]–[79] and the spatially resolved steady-state DRS [80]–[82]. To get more in depth, the IS and the spatially resolved based DRS techniques use continuous-wave (CW) illumination sources and a spectrophotometer for measuring the back-reflected spectra. DRS systems are advantageous in measuring the tissue's optical properties, due to their simplicity, compactness, and low cost.

For instance, a recent study proved that IS-DRS system can be built with low costs while being efficient and simple to construct as shown in Figure 4 [17]. The same setup was used in a clinical study to detect the temporal development of skin erythema via computing the erythema index. Figure 5 displays the computed erythema indices in the study, based on the measurement of the daily skin diffuse reflectances in cancer patients. Based on the computed erythema index, DRS was able to detect the patients' skin color change earlier than visual assessment, however, both techniques were done synchronously [17]. Over and above, the acquired DRS data were able to quantify skin erythema via estimating the apparent concentrations of skin chromophores during radiation treatment [17]. In sum, the simple and affordable IS-DRS system succeeded to properly detect and precisely quantify radiation dermatitis during cancer treatment before visual detection by radiotherapists was possible. Unfortunately, DRS measurement techniques can only be used for relatively small ROI inspections with a low demand for spatial resolution. Moreover, it requires direct skin contact, which in some cases (dry and wet desquamation, burns) is hard to achieve.

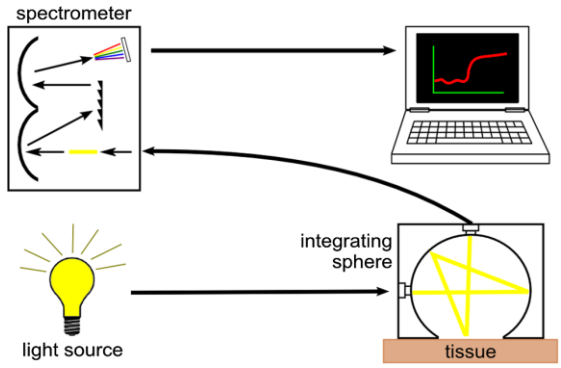

Figure 4: An inexpensive integrating sphere-based diffuse reflectance spectroscopy (DRS) configuration used for skin erythema measurement. The system is composed of a simple wide band light source coupled to an integrating sphere which connected to a PC controlled spectrometer [17].

Unlike both IS and spatially resolved DRS techniques, the time domain (TD) based techniques utilize pulsed light for illumination and detect the skin's back reflection on a temporal basis. Moreover, in order to work properly, the source-detector displacement in TD-DRS techniques should not exceed a couple of centimeters range [83]. To put it simply, the TD- DRS based techniques depend on sending a light pulse to the tissue and detect the back reflected return. Due to the tissue's optical properties, the reflected light pulse is modified in shape and attenuated in amplitude [84]. Based on the detected light pulse envelope modification and the amplitude decrement, the tissue's optical properties is estimated.

Contrasting TD-DRS, the corresponding frequency domain (FD) techniques of diffuse reflectance measurement utilize an amplitude-modulated light source and detect the phase and the amplitude modifications at one or more ROI sites. Reduced sensitivity to noise and straightforward optical implementation are the strong advantages of FD-DRS. Moreover, FD-DRS systems' reliability in data analysis is significantly larger than the corresponding TD-DRS techniques [85].

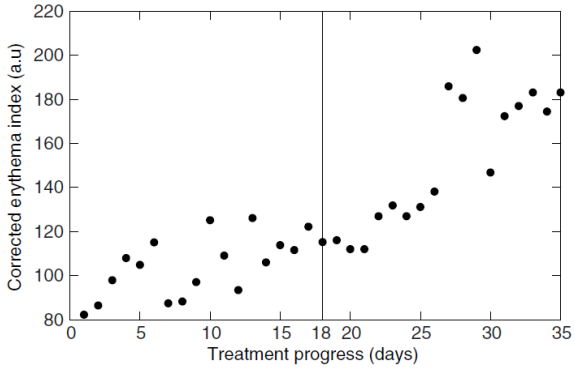

Figure 5: An illustration of the computed melanin-corrected skin erythema index on a daily basis during radiotherapy. The vertical black line at the 18th day indicates the first day for the skin erythema to be clinically observed by visual assessment [17].

Laser Doppler Flowmetery (LDF) is also known as laser Doppler velocimetry. LDF is an optical technique which enables measuring the speed of a moving fluid. The fluid speed is computed via detecting the induced frequency/ Doppler shift in a crossing laser beam. In the context of skin erythema, the moving red blood cells inside the superficial skin vessels cause a Doppler shift, by which erythema could be quantified. Since the erythematous response was originally interpreted being dependent on vasodilation of microcirculation [15], [86], [87]. Although LDF technique looks harmonious for erythema quantification, a past study reported its lower sensitivity in evaluating the UVB-induced erythema. The study supported its report by comparing the Minolta colorimeter and the spectroradiometer [38]. It explained that the blood perfusion's relative change measured by the LDF is not as well correlated with the skin color change as it is in diffuse reflectance spectra [38].

2.4 Imaging-Based Assessment

Imaging was explored as an alternative to overcome the limitations of the spectra-based measurement techniques, including direct skin contact, limited ROI investigation, and local region possible misguidance. Since imaging-based techniques are contact-free, and applicable to examining larger ROI. For instance, LDF were substitited partially in novel applications of laser Doppler imagers (LDI's). LDI's are equipped with a CCD camera, through which false color images for the region of interest can be produced. Thus, the induced minimum erythema discernible (MED) becomes easier to visualize, as shown in Figure 6 [66]. Despite the advanced display in LDI, it is still limited to a small area of investigation. In addition, it lacks the precision of erythema quantification. To increase the area of investigation, digital imaging was the gate.

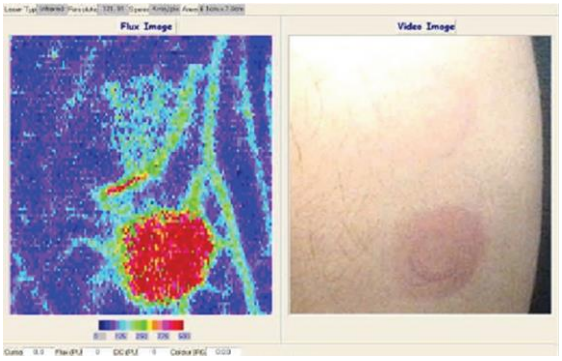

(a) (b)

Figure 6: (a) Laser Doppler imager (LDI) captures images for human skin after applying two different doses of UVB irradiation, and erythema was induced. (b) the corresponding color image of the induced erythema [66].

Digital Color Imaging and Photography is a well-suited approach to surmount visual assessment inter/ intra-observation particularity. It also beats the limitation of the memory of the dermatologist who struggles to retrieve the condition/s of the patients in former sessions. In burns, digital photography spares sensitive skin regions from any contact-analysis during clinical work or research studies [88]. Taking all together, the former advantages, of digital imaging, provides a good opportunity for conducting more research on lately emerging topics. This opportunity is supported by the current technological breakthroughs in electronics, communication, and photography at low cost. For instance, digital imaging, amongst others, have progressive capabilities including (1) autonomous color correction, (2) huge data storage, (3) wireless transfer of images via Bluetooth, and WiFi, and (4) autofocusing. Similar to hardware development, innovations in image analysis/ processing engendered significant steps in registration, feature extraction, and classification.

As such, digital imaging becomes a low-cost portable solution not only for skin pigments quantification [89]–[93], but also in diagnosis of other cutaneous diseases [94]. In support of high dynamic imaging, four factors need to be attentively considered: (1)

illumination, it is necessary to be relentless in intensity and spectra; (2) optimized selection of patient poses, as the skin is highly scattering tissue [90]; (3) the use of auxiliary tools such as special lenses, strong flashlights, spectral band filters, and color checkers, provide the optimal conditions for imaging; and (4) intellectual image analysis algorithms need to be developed, in order to retrieve embedded information inside the captured images. Over and above, individual skills and intermittent training for the photographer play a serious role in producing informative photos. To enhance the image quality, modern technologies provide highly precise and automated photographic apparatus like the one shown in Figure 7, nonetheless they are eminently expensive.

Figure 7: An example of a high-end facial skin imaging station equipped with multiple illumination styles and a ready-made skin analysis software tool used for facial skin inspection [91],[95]. The equipment is immensely expensive due to its independence on human skills in imaging.

Regarding skin erythema imaging, Sergio Coelho et al. [96] reported the feasibility of using digital photography to quantify skin erythema induced by long-term UV exposure. The study employed a digital color image analysis algorithm named "CADIE" to evaluate the skin's erythematous response in volunteers of different backgrounds based on CIELab color system as shown in Figure 8. The study was able to monitor the severity of skin erythema induced by excessive exposure to multiple units of UV radiation. The UV radiation unit is defined as the dose linked to MED. However, MED is an property unique to an individual's skin type and physiology. Albeit all the challenges faced the study, the use of CADIE algorithm enables better identification of skin color changes in terms of Δa* relevant to the received MED units. In spite of this efficacious work, it is important to note that photography loses clarity in revealing tissue surface/subsurface details, wheras polarization does not. Accordingly, polarized light imaging was the key solution to retrieve the lost lucidity.

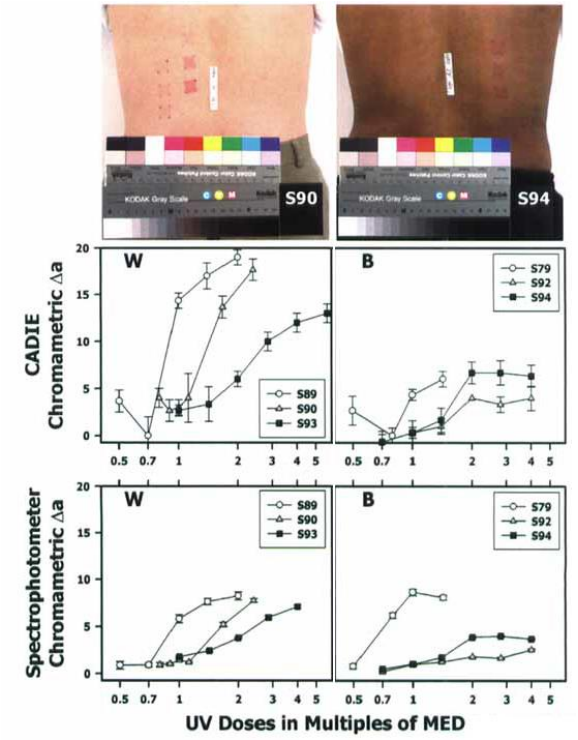

Figure 8: An illustration of the erythematous response in distinct backgrounds (W for white, A for Asian, B for African American) volunteers. The top row, color photos of ROI in one subject from each group of the formerly mentioned backgrounds. The middle row, the relationships detected between the dose of UV radiation expressed in MED units (MED unit is the minimum required UV dose to induce a discernible erythema on the skin of a volunteer) and CADIE-assessed red-green axis Δa* after 1 day of UV exposure. The bottom row, the same relationships are computed based on DRS system using a spectrophotometer. [96]

Polarized light imaging provides the opportunity to selectively acquire information from the tissue's ROI surface and the underneath layers [97], [98]. The former opportunity is based on the fact that the light reflected back out of any tissue's surface, in the case of linearly polarized illumination, is composed of two components. The first of which, specular reflection, probes for the tissue's surface and texture. This component retains the clone polarization type as the incident illumination. In contrast, the second reflected component, diffusely reflected light, does not conduct the same illumination polarization. The loss of polarization is accredited to the scattering interaction of photons beneath the tissue surface, before the

photons bounce back. Therefore, the two components reflected from tissue can be polarly distinguished. To do that, a linear polarizer needs to be installed and selectively oriented ahead of the imaging detector. For surface information acquisition, the linear polarizer should be matched to the incident illumination polarization direction. To exclude surface data, orthogonal polarization to illumination's one has to be chosen. In an erythema framework, polarized imaging improved the skin redness visualization in acne lesions [89]. Furthermore, improved contrast was reported as a benefit of polarized imaging in monitoring the microcirculation, vasodilation, and vasoconstriction as shown in Figure 9.

Inspired by the considerable improvement achieved by polarized imaging, a recent study claimed that linear, elliptically polarized light imaging is also a potential approach for enhancing the contrast and the resolution depth of captured images [99]. Although polarized imaging did a great job in visualizing particular polarization oriented tissue features, other tissue symptoms still can not be elucidated except if excited earlier, as in fluorescence imaging.

Fluorescence imaging detects prompted emission, and mainly fluorescence, as it may be more valuable than absorption property in scaling molecules [100]. Fluorescence imaging procedure depends on a limited spectral band for both excitation, and detection. Filters/ monochromators are always incorporated in the optical path to ensure only excitation and emission bands are transmitted. Fluorescence measurements of the human skin are frequently done using optical fibers since excitation and emission bands are easily separated [37]. In general, the involved fiber bundle, in measurement, is divided into two pathways: one to deliver the excitation light while the other pathway is to collect the skin emission.

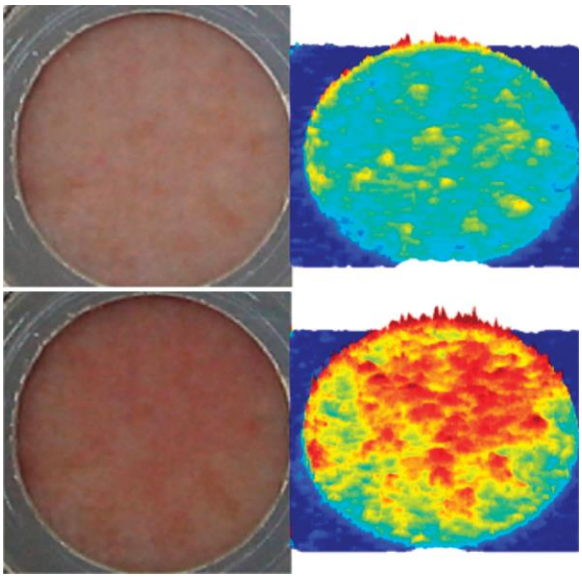

Figure 9: The top row, the normal skin image, for a bounded region, is displayed captured with digital photography on the left and with spectroscopy details on the right. The bottom row shows the same region of interest images, by both photography and detailed spectroscopy, however, showing the effects of using a vasodilator drug, induced by iontophoresis. Polarization spectroscopy imaging proved to be more efficient in displaying the heterogeneity of the microvasculature over the whole studied region of skin [101]

Considering skin as a sample, the chromophore, melanin, significantly absorbs light in the wavelength range 340:400 nm and absorbs relatively less light in the emission bands 360:560 nm [102]. The optical properties of melanin provide fluorescence imaging with a good likelihood to identify the highly concentrated regions of the chromophore distribution within the skin. In the context of erythema, fluorescence imaging was used in a couple of studies, for examining post-inflammatory hyperpigmentation (PIH) related to acne lesions and monitoring superficial acne spot development due to courses of treatment [103], [104].

A simple schematic diagram for fluorescence imaging optical configuration is shown in the top row of . The figure illustrates the basic setup of fluorescence imaging. A wideband light source is (xenon in this case) filtered to excite the tissue under investigation. The prompted emission of the excited tissue is filtered by an emission filter and then imaged using a camera sensor.

In Figure 10, the middle row shows two photographic pictures for a patient who has facial acne lesions before and after 12weeks of treatment. The bottom

row displays the same patient's fluorescence images at the formerly mentioned time points. By image analysis, the study, to which the images belong to, proved that fluorescence images of the patient were more capable of highlighting the facial erythematous regions' modified due to the used treatment in contrast with regular photography [104]. Even if fluorescence imaging is required to show molecular scale particles in biological tissue, it is neither the safest approach nor the only way to achieve such information. For instance, microscopic imaging is also intertwined with erythema assessment in order to create a deep understanding of the linked tissue microstructure.

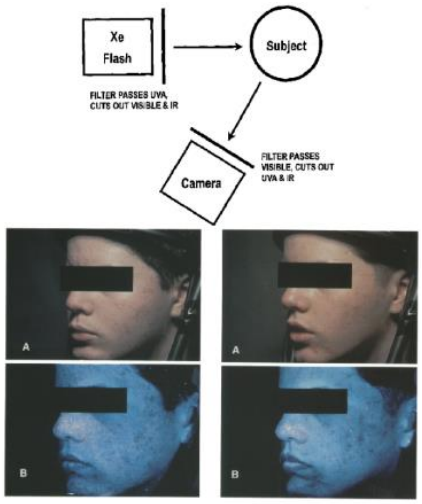

Figure 10: Top row, a schematic diagram of a fluorescence optical imaging configuration. Middle row, an acne patient's images with flash photography is displayed at week-1 (left) and week-12 (right) of acne treatment. Bottom row, the images of the same patient, at the same weeks of treatment, however, captured by fluorescence imaging configuration are shown. The fluorescence images were delineating the acne lesions in the face more clearly than traditional photography [104].

Microscopic imaging is an approach to exploring skin diseases associated with erythematous signs at the cellular scale of resolution. Microscopic imaging enhances the assessment accuracy of the skin's inflammatory regions by permitting the visualization of the detailed structures encompassed in the skin layers. For instance, the stratum corneum and dermoepidermal junction is difficult to visualize using macroscopic imaging, and instead requires microscopy. It is interesting how much details can be revealed with a microscope like Dermoscopy. For example, Dermoscopy is capable of disclosing three distinct skin properties: architecture, pigmentation, and divergent regions' perimeters. As a consequence, it provides a great opportunity for physicians to interpret rare dermatological features [105].

Confocal microscopy is a distinguishable functioning microscopic imaging configuration [106]. It is capable of resolving microanatomic structures within the skin to a near histological resolution [107]. For instance, confocal scanning laser microscopy brings to the dermatologist's eyes detailed skin structure without the need for biopsy. This scale of resolution is very explnatory in skin diseases including contact dermatitis, as shown in Figure 11 [108], [109].

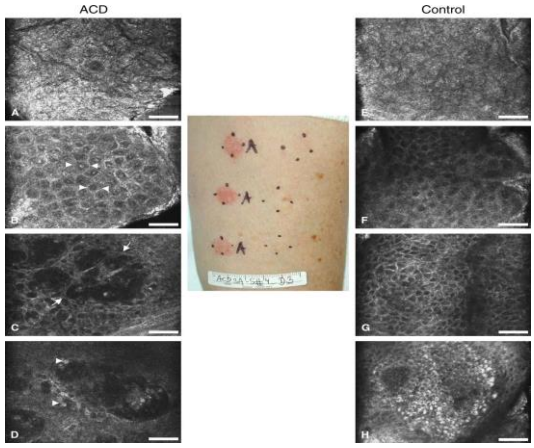

Figure 11: Sections of skin diagnosed with allergic contact dermatitis (ACD) and other sections for control healthy skin regions, where the confocal microscopy images show the differences in the skin structure between ACD skin regions and the normal ones at a near-histological level of resolution [108], [109].

Confocal microscopy is comparable both histology and patch testing, in diagnosing and monitoring allergic contact dermatitis (ACD), due to its high sensitivity and specificity in detection [110]. Although dermatological microscopy offers high resolution, it has some disfavors. The disfavors of microscopy are: (1) the instruments are bulky, which makes it difficult to transport; (2) pricey, thus it is not affordable in small dermatological clinics; and (3) most of the time invasive, thus inconvenient for patients; and (4) time-consuming.

A less expensive, yet still highly informative technique is spectral imaging. Spectral imaging is an emerging technique because of its capability of acquiring a wealth of information in both the spatial and the spectral domains.

Spectral Imaging (SI) is an imaging technique in which multiple frames are taken for the object of interest, like in photography, however, at distinct wavelengths. Thus, the total spectral radiance of the object is acquired. SI generates a 3-dimensional data set, one dimension is spectral and the rest is spatial. Different names are given to SI such as imaging spectrometry/ chemical imaging [111], [112]. A list of parameters are utilized as basis for SI classification including the number of bands, resolution, and acquisition schemes.

Data acquisition in SI is accomplished via different ways including scanning (spectral or spatial) and non-scanning (snapshot) techniques. To give an example, the spectral scanning technique is dependent on involving optical filters which might be static or tunable filters. The tunable filters (TF) scan the spectra with high resolution and does not produce vibration in a very short time. These advantages allow the TF-SI to dominate in SI configurations. Two famous examples of tunable filters are; acousto-optic (AOTF) or liquid crystal (LCTF). SI, in general, imposes the use of broadband light sources that produce a broadband of emission, such as tungsten-halogen or xenon lamps. This emission is sliced and detected by a monochromatic CCD or CMOS sensor.

Regarding SI number of bands, for example, there are three classes; multispectral imaging (MSI, usually uses less than 10 bands) [12], [113], [114], hyperspectral imaging (HSI, > 10 and < 1000 bands) [115]–[117], or ultraspectral imaging (USI, ≥ 1000 bands) [118]. For the sake of convergence, only HSI will be discussed.

HSI produces a datacube that holds a wealth of information. This wealth of information offers a potential solution to arduous obstacles in a sundry of applications [119]. To give an example, HSI was used to address many challenges in the medical field as reviewed elsewhere [120]. Particularly, HSI is a technique of great potential for skin erythema assessment because it is contactless, objective, suitable for wide area imaging, and capable of mapping chromophore distributions. Taking all these reasons into account, HSI is likely an excellent candidate for skin erythema quantitative assessment.

The challenge of objectively quantifying skin erythema that is non-homogenously distributed over a wide skin region can likely be resolved with a technique which combines the advantages of imaging and spectroscopy in one equipment. This equipment should perform hyperspectral imaging and produce spectral-spatial datacube. The intellectual analysis of the produced datacube enables mapping of the skin color changes relevant to the induced erythema, as wekl as calculating the apparent concentrations of the skin chromophores [121] [122]. HSI has been used in literature to delineate the variable intensities of skin erythema accompanied by a few skin problems [122]–[126]. For example, HSI was capable of mapping acne lesions, the skin's viral infections, and contact allergic dermatitis, which are associated with erythematous signs as well as erythema temporal evolution [127]. Morever, HSI is more proficient at mapping the erythematous skin regions in terms of contrast, compared to red-green-blue (RGB) digital imaging.

A schematic diagram and implementation of a recently developed multiview HSI [128] used for studying the tissue structure and its functional attributes is shown in Figure 12. The novel multiview capability of HSI enabled the operator to outline the topography of a wound associated with erythematous regions. In addition, it facilitates the construction of a 3-dimensional image as shown for a wound model in Figure 13 [128].

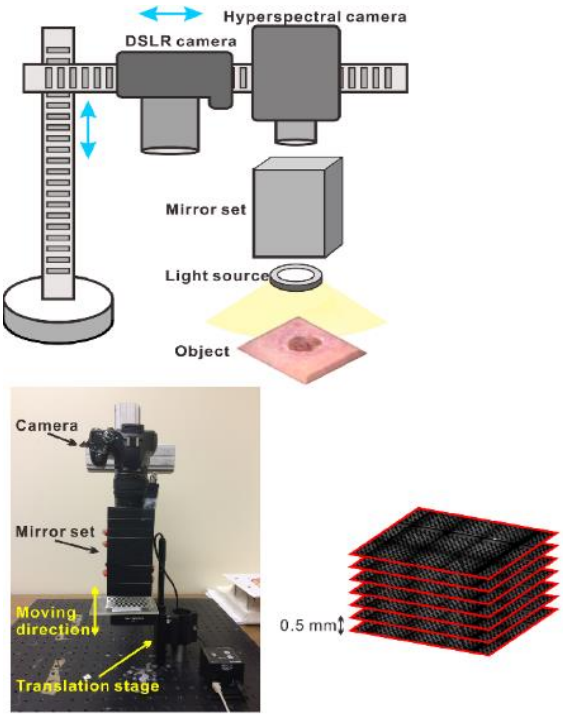

Figure 12: Multiview HSI schematic diagram, laboratory implementation. The system is composed of two cameras; one is digital and the other is spectral, where both cameras are moving along a horizontal arm for positioning and the horizontal arm is leveled vertically with a step resolution of 0.5 mm. A mirror set is integrated between the object and the spectral camera to enable Multiview process [129].

Several studies ([93], [130], [131]) put an effort to obtain the erythema maps from RGB images; however, the quality of these maps was very limited [132]. The former limitation was attributed to the skin's optical properties which are spectrally dependent on the encompassed chromophores (both types of hemoglobin, melanin, water,…). Therefore, it becomes difficult to optically monitor and precisely quantify the chromophores concentration alterations using only red, green, and blue channels in photography. As a result, HSI is tagged the "gold standard" for skin erythema mapping [132]. Added to mapping, HSI has an impressive sensitivity to detect the onset of erythema before it becomes visible to the clinician eye [132].

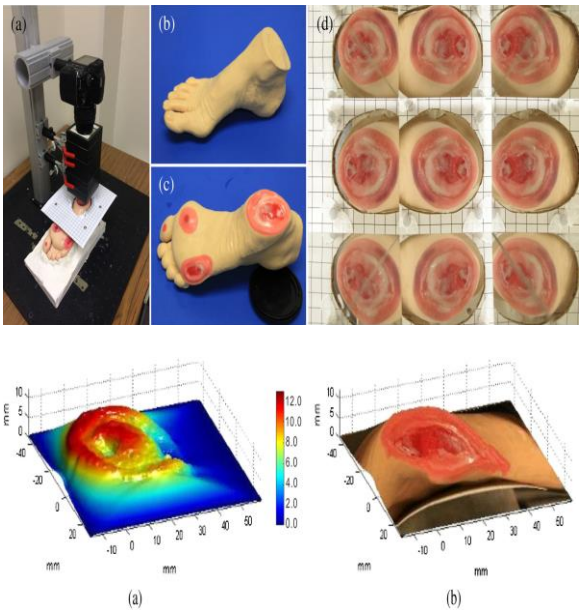

Figure 13: Top-row, (a): Multiview-HSI system (b, c) the foot wound model, (d) digital color pictures taken by the Multiview modality. Bottom-row, (a) 3-D wound model topology built from the Multiview hyperspectral captured frames, (b) and the corresponding digital color 3-D wound model. [128]

3 Other Assessment Techniques

This section is dedicated to presenting an overview of the less frequently utilized techniques for skin erythema assessment including optical coherence tomography, ultrasound imaging, magnetic resonance imaging, and dielectric constant measurement. The reasons for the low popularity of these techniques are diverse. For instance, these techniques are disfavored by lower sensitivity, higher cost, complexity, substantial size and weight, mobility problems, or a combination of the above.

3.1 Optical Coherence Tomography (OCT)

OCT is an optical technique that makes use of the interference of coherent light. To put it simply, OCT imaging uses a Michelson interferometer, as shown in Figure 14 top-row [133]. The information in OCT stems from the interpretation of the interference pattern generated by a low coherence laser beam. The laser beam in OCT configuration is split into two rays, one of which is directed to the sample and the other is guided toward a mirror. In-phase interference generates bright fringes, constructive interference, and dark fringes, destructive interference. The laser's short coherence length permits the determination of the

penetration depth: images from subsurface layers can be drawn in analogy to A-scans in ultrasound [37]. While B-scans in OCT are formed by the combination of fringe intensities in adjacent A-scans.

In the past, OCT required a long time to build a tissue image due to its slow scanning techniques. Real-time imaging is now possible [134]. The penetration depth of OCT is mainly dependent on the laser's central wavelength. For example, the NIR wavelength of 1300 nm leads to a penetration of about 1.2 mm in comparison with 0.7 mm using light in the 700 nm red region. The typical lateral resolution may vary between 10-15µm, however, there are some special techniques that can lead to 1-3µm penetration, entering the region accessible by confocal microscopy [133]. OCT has the feasibility to detect the presence of skin diseases associated with tenderness and erythema. OCT's detection of erythema is observed on the interference built images in the format of increased thickness in the epidermal layer, reduction in light scattering, and a dilated vasculature network [135], as shown in Fig.14 bottom-row [134]. Although some OCT systems are currently available as bench-top devices, their sensitivity is utterly vulnerable to change in the case of slight movements during in vivo measurements. These unintentional movements of patients result in blurry images [134]. Two major differences exist between OCT and ultrasound: need for skin contact and the sensitivity to patient movement.

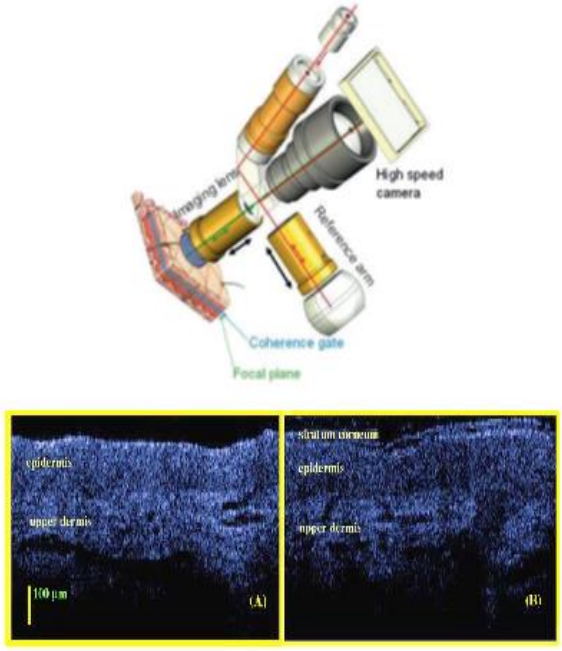

Figure 14: (top) Schematic diagram of a high definition OCT (reproduced from [133]), (bottom) 2D-OCT scanned images of human back skin before (left) and after (right) UVB irradiation; after radiation, the stratum corneum is separated from the subsurface layers and the light intensity is reduced [134]

3.2 Ultrasound-Based Imaging

Ultrasound, like OCT, is supplementary equipment in the dermatological bench-top instrumentation. Ultrasound became a tool to measure the skin thickness since the last quarter of the 20th century [136]. Following that, ultrasound imaging expanded to different dermatological issues, including skin irritation and erythema [137]–[141]. The basic principle of ultrasonic imaging is detecting the reflected acoustic waves exiting from the different layers within the tissue of interest. The tissue components are quite often different in density and hence they respond to the transmitted acoustic waves individually. Distinct responses, from the different layers of the scanned tissue to the acoustic waves, are transformed and displayed on the ultrasound monitor as an image of the tissue's underlying structure represented by gray scale intensities [142]. A wide range of acoustic frequencies is used in ultrasonic imaging, where lower frequencies are used to visualize deeper structures in tissue. Examples of the used frequencies are shown in Table 2 [142]. In advanced ultrasonic imaging, the system is not only imaging stationary structures but also monitoring the moving

fluids like arterial/ venous blood by adopting Doppler ultrasound methodology.

Table 2: Ultrasonic imaging frequencies and associated penetration depth within visualized skin part [142]

Ultrasonic freq. (MHz)	Visual skin part	Penetration depth (cm)
7.5	Lymph nodes	~ > 4.00
13.5-50	Dermis and epidermis	~ 3.0:0.3
20	Dermis and epidermis	~ 0.6:0.7
50-100	Epidermis	~ 0.3:0.015

Ultrasonic imager is a noninvasive and portable device, used to measure the tissue thickness within the lesions area. The tissue thickness was found to be inversely proportional with skin erythema. This relationship between the skin thickness and the skin erythema due to irradiation was verified in a breast cancer study [137]. Another study showed the productive usage of ultrasound in imaging a forearm dermatofibroma nodule surrounded by an erythematous region. The nodule was imaged, blue dot, before the removal surgery (see Figure 15 [143]) to alert the surgeon of the nearby vein. Although ultrasound was able to quantify erythema indirectly via skin thickness measurement, a contradicting study showed that an acoustic equipment was less efficacious at assessing erythema [67]. The contradicting study measured skin thickness using an ultrasound-based device, and showed a low correlation between both the melanin and erythema indices. Hence, the study concluded that skin thickness is not a productive measure of assessing subcutaneous fibrosis and the componential changes of the skin parenchyma Therefore, ultrasound is an inadequate technique for studying skin erythema associated with different cutaneous diseases in contrast with, for example, spectral based modalities.

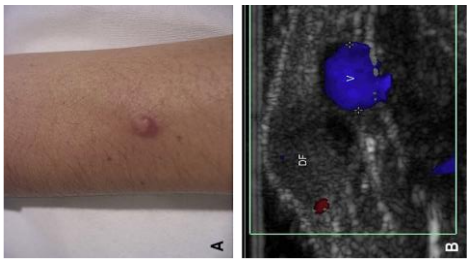

Figure 15: An illustration of Dermatofibroma (DF) case inspected by ultrasound instrument: (A) forearm erythematous nodule, (B) Ultrasonic transverse view image displays erythematous nodule near a large vein (blue spot) which assist in being avoided in surgery. [143].

3.3 Magnetic Resonance Imaging (MRI)

MRI is a distinguishable imaging technique by which high spatial resolution images for minute tissue components can be acquired [144]. Such highly sophisticated imaging modality is not commonly used for superficial skin disorders. However, in a previous study, MRI was used toward 3-D mapping of acne lesions and psoriasis as shown in Figure 16 [145]. The major disadvantages of such high-resolution imaging modality are; the big size, the technical complexity, and the instrument high costs.

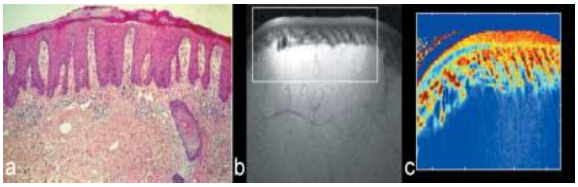

Figure 16: (a) Histological image of a severe psoriasis case, (b) anatomical view with the marked region of interest (ROI), (c) a relaxation time T1 map calculated for the ROI, where the increased red color intensity in the outer dermis layer is due to the skin inflammation [145] .

3.4 Dielectric Constant Measurement

Dielectric constant measurement is used in diverse medical applications as reviewed elsewhere [146]. Regarding the skin, dielectric constant measurement was utilized to detect the reactions induced by irradiation in breast cancer radiotherapy treatment [147]. The basic way to measure the dielectric constant of the skin is to connect an open terminal coaxial probe to a network analyzer. The probe functions to transmit electromagnetic (EM) waves at harmless frequencies through the skin's ROI and to measure the return signal through the network analyzer. It has been reported that the dielectric constant is inversely correlated to the clinically scored erythema [147]. Hence, dielectric constant measurement proved to be an objective method of noninvasively quantifying skin erythema. Nevertheless, the skin variability between people and the inconsistent dielectric properties in the same person yield less repeatable results. Therefore dielectric constant measurement was less credible for clinicians to use in their daily practice.

4 Erythema Indices

This section briefly introduces the different computation approaches for the skin erythema index through a review of the literature. The purpose of this review is to hand over a synopsis of the skin erythema index calculation in order to encourage more studies to validate and compare them [148]. This comparison helps to identify the optimal skin erythema estimation method.

4.1 Dawson Indices

The use of Dawson indices is a familiar approach for quantitative estimation of the skin color changes due to a disease's development [149], or a medical treatment [68]. Dawson derived his erythema index (DEI) formula based on the assumption of a proportional relation between the hemoglobin optical absorption in the range of 510-610 nm and the erythema scores. Dawson found that the area under the curve for the hemoglobin absorption, if a baseline is determined, is the parameter related to the skin erythema variation and calculated as follows:

$$\mathrm{DEI} = 50 * [2r + 3(q + s) - 4(p + t)] \quad (7)$$

The terms, p, q, r, s, and t are the symbols expressing the logarithm of the reciprocal of the reflectance (LRR) measured at five predetermined wavelengths 510, 540, 560, 580, and 610 nm, respectively. Dawson melanin index (DMI) is computed based on two central wavelengths (650 and 700 nm). As it is assumed that melanin concentration is relative to the slope of the skin spectral curve of absorbance ($A_{xxx} = \log_{10}\frac{1}{R_{xxx}}$) bounded by the two formerly mentioned wavelengths. The formula used for computing melanin index is the average of the skin absorbance values for two wavelengths surrounding 650 nm and 700 nm ($\lambda \pm 5$ nm) as seen in equation 8:

$$\mathrm{DMI} = (100 * [\log_{10}\left(\frac{1}{(\bar{R}_{645,650,655}}\right) - \log_{10}\left(\frac{1}{(\bar{R}_{695,700,705}}\right)]) + 1.5 \quad (8)$$

The term R_{xxx} is the computed reflectance at certain wavelength xxxin nanometers. The constant at the end is an empirical correction constant. The DEI can be corrected ($\mathrm{DEI_c}$) using the DMI by applying the formula as shownin equation (9), where $\gamma = 0.04$ is an empirically derived balancing constant by Dawson to avoid negative values due to the existing while being insignificant skin chromophores:

$$\mathrm{DEI_c} = (50 * [2r + 3(q + s) - 4(p + t)]) * (1 + (\gamma * \mathrm{MEI})) \quad (9)$$

Subsequent reflectance measuresments are taken to evaluate response to pharmaceutical treatment of a cutaneous disease. Following the masurements, Dawson's relative erythema index ($\mathrm{DEI_r}$) is computed to assess the skin color change. The term $\mathrm{DEI_r}$ is basically equivalent to the difference in value between $\mathrm{DEI_c}$ for two skin sites, one of which is the treated site while the other is the control (non-treated) site.

4.2 Diffey Index

Diffey index [62] was built on a simple observation of hemoglobin absorption attributes. Diffey realized that hemoglobin absorption is higher in the green spectral region than the corresponding red region. Based on this realization, Diffey proposed an erythema index by computing the ratio of the inverse logarithm of the skin spectral reflectance at two wavelengths: green (565 nm) and red (635 nm). Diffey didn't correct for the melanin effect in his computation. The formula which expresses Diffey index is given in equation 10.

$$E_{Dif} = -\log_{10}\left(\frac{R_g}{R_r}\right) \quad (10)$$

4.3 Tronnier Index

Tronnier [150] had a similar approach to erythema computation as Diffey [151]. A difference is that Tronnier principle computes the relative rather than the absolute erythema. Consequently, he created his index ($\mathrm{E_T}$) based on a study. The study focused on the skin color change due to UV-irradiation induced erythema (Er) versus a control (C) region. Tronnier, unlike Diffey, accounted for melanin in his computation. However, he assumed that the relative calculation should compensate for the melanin absorption in the skin tissue without the need for a separate calculation step. In summary, he used the back reflected light measurements at two wavelengths: 545 nm and 661 nm for both the erythematous ($\mathrm{Er_g}$,

Er_r) and the control regions (C_g, C_r) to assess the skin's relative erythema, as shown in (11).

$$E_T = ((Er_g - Er_r) - (C_g - C_r)) \quad \textbf{(11)}$$

4.4 Ferguson-Hemoglobin Content

Ferguson developed another computation technique for skin erythema called the index of hemoglobin content (IHB) [152]. The developed technique depends on the use of the isosbestic absorption points of hemoglobin both components (i.e. spectral points of equal absorption for the oxygenated and deoxygenated components of hemoglobin). These wavelengths are the core input data for IHB computation. The term OD_{xxx} is the optical density of the skin at certain wavelengths of *xxx* nanometers.

$$\text{IHB} = \left[\left({}^{1}/_{16.5} * (\text{OD}_{544} - \text{OD}_{527.5}) - {}^{1}/_{29} * (\text{OD}_{573} - \text{OD}_{544})\right] * 100 \quad \textbf{(12)}$$

4.5 Hajizadeh Method

Hajizadeh conducted two studies [153], [68] taking into consideration the melanin absorption effect on the measurement of the backscattered light from the epidermis layer. The two studies paid more attention to highly pigmented participants versus light skinned participants. To this end, the melanin index M_{675} was computed as shown in (13) based on the absorption curve region, similarly to Dawson's method [154]. However, Hajizadeh had proposed a new compensation factor due to a synthetic melanin absorption measurement. This measurement is equivalent to the *in vivo* one, and thus he had developed the term named after him, M_H, which is expressed in µg/cm^2 as shown in (14).

$$M_{675} = 100 * \left\{\frac{OD_{700} - OD_{650}}{50} + \left(0.06 * \left[\frac{1 - SaO_2}{100}\right] + 0.01\right) * IHB/80\right\} \quad \textbf{(13)}$$

$$M_H = (54 * 10^{-3} - M_{675}) * 120.1) \ \mu g/cm^2 \quad \textbf{(14)}$$

Using the newly developed melanin index, M_H, the "true" hemoglobin content can be computed. This is done by applying an empirical constant as shown in (15):

$$IHB_{true} = IHB_{cor} + 0.000047 * M_H \quad \textbf{(15)}$$

4.6 Helen Hayes Hospital

Helen Hayes Hospital (HHH) method is an approach of quantifying erythema mentioned elsewhere [148]. HHH uses an *in vitro* measurement for a standard melanin sample as a reference. The reference sample absorbance is tunable to match the individuals' skin melanin content within the spectral range 500-625 nm. This method has the advantage of consistency for both high and low pigmented skin. However, this method has a shortcoming due to its impotence to physiologically interpret the melanin content changes between the different locations in the same person, for example between an erythematous and a control skin region [148].

5 Discussion

No doubt, VA is still the gold standard [97] and the primary method for skin erythema assessment. It has not yet been supplanted by any other methods . As a proof, a study [155] provided evidence of imprecise spectrometer results compared to the clinical visual assessment. Figure 17, belongs to this study, and shows that the erythema index (d IE) is inconsistent with a clinical assessment of formaldehyde-induced erythema [155]. It is of interest to mention that VA is not perfect since it has critical shortcomings. Primarily, VA is based on a subjective perspective, and thus suffers from inter- and intra-observation individuality, as well as dependency on scene conditions. Secondly, the therapist eye is capable of detecting the difference between the skin colors, but it is unqualified to designate an absolute value for the detected color difference. Moreover, VA is poor in prescisely delineating the margins between distinct erythematous levels. Another point of critique against VA is color blindness, which may exist undeclared among clinicians [156].

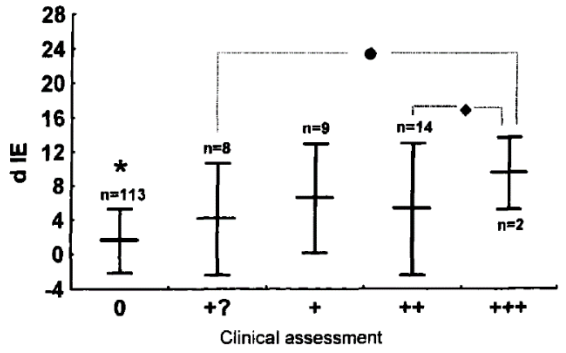

Figure 17: Comparison between the Dermaspectrometer delta erythema index (d IE) and the clinical assessment of formaldehyde patches applied to patients' skin. The term d IE is equivalent to the difference between the erythema reading of the Dermaspectrometer acquired for ROI and a control region. The horizontal axis is the clinical skin erythema score which ranges from 0 for normal skin and +++ for severe skin erythema. The vertical axis is the erythema index score. The term (n) is the number of people who have the same reaction, the (*) sign is indicating high correlation with positive patch test ($P<0.05$, ANOVA test), and the sign (♦) is pointing to separable categories ($P<0.05$, ANOVA test) [155].

To overcome the low precision of the therapist eye, inexpensive and portable color charts are used as a supplementary tool. They help the clinician to document the color tone of the skin, a quality that is hard to remember and to communicate verbally. Although color charts reduced the limitation of VA, they still suffer from individualism and durability. In addition, color charts are vulnerable to metamerism, which is the inconsistent matching of two colors as a result of certain conditions including illumination type, geometrical position, and human-to-human color detection acuity.

Going far from subjective means, tristimulus instruments opened the gate for objective assessment for skin pigmentation. However, these devices are heavy and pricey as well. Hence, these devices failed to achieve popularity in clinics. In terms of size and weight, the narrowband devices, Mexameter and Dermaspectrometer, garnered some interest from clinicians. Nevertheless, the narrowband devices are poor at distinguishing between different skin types since their operation is dependent on limited wavelengths. One more limitation of the former devices is the need for skin contact. This contact does not only limit their use in sensitive regions including burns, but also renders them susceptible to stuck with local skin variations due to the limited region of inspection.

The spectral limitation of the tristimulus, and the narrowband devices was the reason behind bringing diffuse reflectance measurement into skin assessment. DRS measurement techniques consequently were utilized to detect changes in skin reflectance as a result of cutaneous disease or treatment. Although DRS measurement techniques are efficient in determining the optical properties of tissues, they still have a few limitations. For instance, the typical IS-DRS configuration has less precision in the spatial domain. Hence IS-DRS becomes challenging in separating the particular influence of scattering and absorption in the absence of a predetermined scattering spectrum for the sample under test [85]. Like IS-DRS, the spatially-resolved DRS is not flawless. It is dependent on a few local point measurements which might yield indecisive outcomes [157]. Far from CW illumination, TD-DRS measurement techniques provide the advantage of acquiring both absorption and scattering coefficients data via a single measurement. Nonetheless, it requires a complex set of pricey instrumentation, which is not available everywhere. The prior DRS techniques disadvantages paved the way for imaging techniques to advance toward skin erythema quantitative assessment.

Digital imaging use in erythema assessment is a tough process because it needs firm constraints in order to obtain informative data. To give a brief, the illumination in digital imaging needs to be securely maintained within the same level of intensity, emitted spectra. For illustration purposes, Figure 18 [91] displays two non-identical pictures of a single patient taken at two different illumination conditions. Although there is no change except in the illumination, the two pictures may be falsely interpreted by the clinician as two distinct skin conditions.

Figure 18: Example of illumination conditions impact on the outcome of photographed pictures, which may lead to an error in clinical diagnosis [91].

To overcome both illumination problems and specular glares, polarized imaging was solicited. However, polarized imaging requires an integration of additional optical components. Such addition of the optical components leads to: first, an increase in the cost of the developed optical setup, and second, growth the system's sheer complexity with respect to setup and alignment. Besides, the greater the number of the integrated optical components in optical imaging, the more intense the illumination and the more sensitive the detector are required.

Although fluorescence imaging has a great potential to display skin structure in the molecular scale, its use is limited due to the possible harm of UV light to the eyes and the skin. In addition, fluorescence imaging requires special tools/ instrumentations, and personal protective equipment for both the patient and the imaging operator, which constitute an overhead cost. For instance, high sensitive detectors are required to detect the low intensities of both the exciting illumination and the fluorescence emission since the band filters or a monochromator are used in excitation and emission.

The microscope is the shortcut technique to extract the root information about skin diseases associated with erythema. Despite this fact, the microscope is not popular since it is expensive, and difficult to move. Moreover, the microscope often requires a skin biopsy for laboratory analysis. Hence, a change of the optical properties may take place during transport of the biopsy sample from the clinic to the laboratory. Coupled with the relatively long time required for lab analysis, microscopy is limited to the analysis of small skin regions. Far from common techniques, OCT, ultrasound, MRI, and dielectric constant measurements, are less attractive for dermatology clinics, due to many reasons such as their size, cost, and inconvenience.

The microscope is the shortcut technique to extract the root information about diseases associated with erythematous signs. Nontheless, the costs and limited portability of microscopes yielded no popularity in skin erythema assessment. Moreover, the microscope often requires skin biopsy for laboratory analysis. Hence, a change of optical properties may take place during transport of the biopsy sample from the clinic to the laboratory. Coupled with the relatively long time necessary for the lab analysis, microscopy is limited to the analysis of small skin regions.

Far from common techniques, OCT, ultrasound, MRI, and dielectric constant measurements, are the least attractive and least common, methods inthe dermatology clinics, due to many reasons such as the size, cost, and inconvenience.

Aside from common and less common erythema assessement techniques, spectral imaging could be an effective assessment candidate. Spectral imaging is a hybrid imaging technique.It combines both DRS and digital imaging, and thus it overcomes the limitations of each individual technique. For instance, HSI is tagged as the gold standard in skin erythema mapping due its distinguished capability of contouring the distinct skin response intensities. Furthermore, HSI datacube analysis enables a precise estimation of the temporal changes of the skin's componential chromophores. However, HSI still requires a reasonable budget, for either case, building a custom-made spectral camera or purchasing a bench-top one. In addition to the required budget for HSI, one more challenge is to develop an intellectual image processing algorithm to achieve an efficient image registration and precise endmembers classification.

6 Conclusion

Optical science and technology have resulted in incredible advances in miniaturizing apparatus and full-systems to facilitate skin erythema quantification.

Handheld colorimeters, single point spectroscopic devices, digital and spectral cameras are now mobile, pocket-sized, and ready to offer objective measures for various skin diseases associated with erythema. Larger imaging devices are equipped with high definition monitors, capable of producing real-time false color images and displaying the skin's epidermal and dermal symptoms. More sophisticated methods, such as confocal microscopy and OCT, offer almost histological spatial resolutions for details of the erythematous skin. This versatile array of objective tools to study cutaneous diseases associated with skin erythema enhances clinical dermatology practice, in terms of both sensitivity and specificity.

However, the capabilities of the expert clinician's eyes remains irrreplaceable for skin erythema inspection. Nevertheless, technology offers a few solutions for eliminating subjectivity and addressing the previously mentioned disadvantages of VA. From an economic perspective, hiring a number of full-time radiotherapists might be more expensive than purchasing a technology in the long run. Therefore, clinicians who are equipped with an advanced technology are able to provide good service for more patients in a shorter peroid of time. From our point of view, HSI, as a developing optical modality, is a promising future candidate to facilitating the work of clinicians. Since HSI is an objective, precise, and contactless approach to skin pigmentation mapping for a sizable tissue region.

References

[1] M. Nischik and C. Forster, "Analysis of skin erythema using true-color images.," *IEEE Trans. Med. Imaging*, vol. 16, no. 6, pp. 711–6, 1997.

[2] G. Marchini, A. Nelson, J. Edner, S. Lonne-Rahm, A. Stavreus-Evers, and K. Hultenby, "Erythema Toxicum Neonatorum Is an Innate Immune Response to Commensal Microbes Penetrated into the Skin of the Newborn Infant," *Pediatr. Res.*, vol. 58, no. 3, pp. 613–616, 2005.

[3] S. L. Brice *et al.*, "The herpes-specific immune response of individuals with herpes-associated erythema multiforme compared with that of individuals with recurrent herpes labialis," *Arch Dermatol Res*, vol. 285, pp. 193–196, 1993.

[4] A. N. BRUCE, "VASO-DILATOR AXON-REFLEXES," *Quat. J. Exp. Physiol*, vol. 6, pp. 339–354, 1913.

[5] H. M. M. T. Lewis, R. T. Grant, "Vascular reactions of the skin to injury, Part X.—The intervention of a chemical stimulus illustrated especially by the flare. The response to faradism," *Heart*, vol. 14, pp. 139–160, 1927.

[6] H. Hönigsmann, "Erythema and pigmentation," *Photodermatol. Photoimmunol. Photomed.*, vol. 18, pp. 75–81, 2002.

[7] K.-S. Suh *et al.*, "A long-term evaluation of erythema and pigmentation induced by ultraviolet radiations of different wavelengths.," *Ski. Res. Technol.*, vol. 13, no. 4, pp. 360–8, 2007.

[8] J. W. Shin, S. W. Yoon, J. B. Jeong, and K. C. Park, "Different responses of the melanin index to ultraviolet irradiation in relation to skin color and body site," *Photodermatol. Photoimmunol. Photomed.*, vol. 30, no. 6, pp. 308–315, 2014.

[9] M. Bodekær, P. A. Philipsen, T. Karlsmark, and H. C. Wulf, "Good agreement between minimal erythema dose test reactions and objective measurements: An in vivo study of human skin," *Photodermatol. Photoimmunol. Photomed.*, vol. 29, no. 4, pp. 190–195, 2013.

[10] L. R. Sklar, F. Almutawa, H. W. Lim, and I. Hamzavi, "Effects of ultraviolet radiation, visible light, and infrared radiation on erythema and pigmentation: a review," *Photochem. Photobiol. Sci.*, vol. 12, no. 1, pp. 54–64, 2013.

[11] B. Jung, S. Kim, Y. Bae, H. Kang, Y. Lee, and J. S. Nelson, "Real-time measurement of skin erythema variation by negative compression: pilot study.," *J. Biomed. Opt.*, vol. 17, no. 8, pp. 81422–1, Aug. 2012.

[12] L. Kong *et al.*, "Single sensor that outputs narrowband multispectral images.," *J. Biomed. Opt.*, vol. 15, no. 1, p. 10502, 2010.

[13] M. Denstedt, B. S. Pukstad, L. a. Paluchowski, J. E. Hernandez-Palacios, and L. L. Randeberg, "Hyperspectral imaging as a diagnostic tool for chronic skin ulcers," vol. 8565, p. 85650N, Mar. 2013.

[14] G. Heyer, O. P. Hornstein, and H. O. Handwerker, "Skin reactions and itch sensation induced by epicutaneous histamine application in atopic dermatitis and controls," *J Invest Dermatol*, vol. 93, no. 4, pp. 492–496, 1989.

[15] W. Magerl, R. a Westerman, B. Möhner, and H. O. Handwerker, "Properties of transdermal histamine iontophoresis: differential effects of season, gender, and body region.," *J. Invest. Dermatol.*, vol. 94, no. 3, pp. 347–352, 1990.

[16] D. E. McKee, D. H. Lalonde, A. Thoma, D. L. Glennie, and J. E. Hayward, "Optimal Time Delay between Epinephrine Injection and Incision to Minimize Bleeding," *Plast. Reconstr. Surg.*, vol. 131, no. 4, pp. 811–814, 2013.

[17] D. L. Glennie, J. E. Hayward, D. E. Mckee, and T. J. Farrell, "Inexpensive diffuse reflectance spectroscopy system for measuring changes in tissue optical properties," *J. Biomed. Opt.*, vol. 19, no. December, pp. 105005-1-105005–6, 2014.

[18] E. Van Den Kerckhove *et al.*, "The assessment of erythema and thickness on burn related scars during pressure garment therapy as a preventive measure for hypertrophic scarring," *Burns*, vol. 31, no. 6, pp. 696–702, 2005.

[19] S. D'haese, M. Van Roy, T. Bate, P. Bijdekerke, and V. Vinh-Hung, "Management of skin reactions during radiotherapy in Flanders (Belgium): a study of nursing practice before and after the introduction of a skin care protocol.," *Eur. J. Oncol. Nurs.*, vol. 14, no. 5, pp. 367–372, 2010.

[20] D. Yohan *et al.*, "Quantitative monitoring of radiation induced skin toxicities in nude mice using optical biomarkers measured from diffuse optical reflectance spectroscopy.," *Biomed. Opt. Express*, vol. 5, no. 5, pp. 1309–20, 2014.

[21] L. Diana L. Glennie, Joseph E. Hayward, Orest Z. Ostapiak, James Wright and T. J. F. Doerwald-Munoz, "Diffuse reflectance spectroscopy for monitoring erythema in head & neck intensity modulated radiation therapy," *J. Radiat. Oncol.*, 2014.

[22] N. Lee *et al.*, "Skin toxicity due to intensity-modulated radiotherapy for head-and-neck carcinoma," *Int. J. Radiat. Oncol. Biol. Phys.*, vol. 53, no. 3, pp. 630–637, 2002.

[23] D. Porock and L. Kristjanson, "Skin reactions during radiotherapy for breast cancer: The use and impact of topical agents and dressings," *Eur. J. Cancer Care (Engl).*, vol. 8, no. 3, pp. 143–153, 1999.

[24] M. McQuestion, "Evidence-Based Skin Care Management in Radiation Therapy," *Semin. Oncol. Nurs.*, vol. 22, no. 3, pp. 163–173, 2006.

[25] J. W. Denham *et al.*, "Factors influencing the degree of erythematous skin reactions in humans," *Radiother. Oncol.*, vol. 36, no. 2, pp. 107–120, 1995.

[26] T. Olschewski, K. Bajor, B. Lang, E. Lang, and M. H. Seegenschmiedt, "[Radiotherapy of basal cell carcinoma of the face and head: Importance of low dose per fraction on long-term outcome].," *J. Dtsch. Dermatol. Ges.*, vol. 4, no. 2, pp. 124–30, 2006.

[27] D. Yohan *et al.*, "Quantitative monitoring of radiation induced skin toxicities in nude mice using optical biomarkers measured from diffuse optical reflectance spectroscopy.," *Biomed. Opt. Express*, vol. 5, no. 5, pp. 1309–20, 2014.

[28] D. Basketter, F. Reynolds, M. Rowson, C. Talbot, and E. Whittle, "Visual assessment of human skin irritation: a sensitive and reproducible tool.," *Contact Dermatitis*, vol. 37, pp. 218–220, 1997.

[29] M. Bruze, M. Isaksson, B. Edman, B. Björkner, S. Fregert, and H. Möller, "A study on expert reading of patch test reactions: inter-individual accordance," *Contact Dermatitis*, vol. 32, pp. 331–337, 1995.

[30] E. Held, H. Lorentzen, T. Agner, and T. Menné, "Comparison between visual score and erythema index (DermaSpectrometer) in evaluation of allergic patch tests," *Ski. Res. Technol.*, vol. 4, no. 4, pp. 188–191, 1998.

[31] S. Wan, J. a Parrish, and K. F. Jaenicke, "Quantitative evaluation of ultraviolet induced erythema.," *Photochem. Photobiol.*, vol. 37, no. 6, pp. 643–648, 1983.

[32] B. L. Diffey and P. M. Farr, "Quantitative aspects of ultraviolet erythema," *Clin. Phys. Physiol. Meas.*, vol. 12, no. 4, p. 311, 1991.

[33] A. S. C. J. Taylor S.C., "The Taylor Hyperpigmentation Scale: A New Visual Assessment Tool for the Evaluation of Skin Color and Pigmentation," *Ther. Clin.*, vol. 76, no. 4, pp. 270–274, 2005.

[34] M. H. Ahmad Fadzil, D. Ihtatho, A. Mohd Affandi, and S. H. Hussein, "Objective assessment of psoriasis erythema for PASI scoring.," *J. Med. Eng. Technol.*, vol. 33, no. 7, pp. 516–24, 2009.

[35] S. Banu, G. Toacse, and G. Danciu, "Objective erythema assessment of Psoriasis lesions for Psoriasis Area and Severity Index (PASI) evaluation," *EPE 2014 - Proc. 2014 Int. Conf. Expo. Electr. Power Eng.*, no. Epe, pp. 52–56, 2014.

[36] A. Raina, R. Hennessy, M. Rains, J. Allred, D. Diven, and M. K. Markey, "Objective measurement of erythema in psoriasis using digital color photography with color calibration," in *Annual International Conference of the IEEE Engineering in Medicine and Biology Society.*, 2014, vol. 2014, pp. 3333–3336.

[37] N. Kollias and G. N. Stamatas, "Optical non-invasive approaches to diagnosis of skin diseases," *J. Investig. Dermatology Symp. Proc.*, vol. 7, pp. 64–75, 2002.

[38] R. M. M. h. A. Lahti, H. Kopola, A. Harila, "Assessment of skin erythema by eye, laser doppler flowmeter, spectroradiometer, two channel erythema meter, and Minolta chromameter," *Dermatological Res.*, pp. 278–282, 1993.

[39] and W. I. l. H. E. L. M. V. Hausser, karl Wilhelm, *Sunburn and suntanning*. London: Pergamon press, 1969.

[40] S. Taylor, W. Westerhof, S. Im, and J. Lim, "Noninvasive techniques for the evaluation of skin color," *J. Am. Acad. Dermatol.*, vol. 54, no. 5, pp. S282–S290, 2006.

[41] I. M. Gibson, "Measurement of skin colour in vivo," *J. Soc. Cosmet. Chem*, vol. 22, pp. 725–740, 1971.

[42] N. Konishi *et al.*, "New approach to the evaluation of skin color of pigmentary lesions using Skin Tone Color Scale.," *J. Dermatol.*, vol. 34, no. 7, pp. 441–446, 2007.

[43] R. G. Kuehni, *Color space and its divisions*, vol. 26, no. 3. Canada: John Wiley & Sons, Inc., Hoboken, New Jersey, 2003.

[44] I. L. Weatherall and B. D. Coombs, "Skin color measurements in terms of CIELAB color space values.," *J. Invest. Dermatol.*, vol. 99, no. 4, pp. 468–473, 1992.

[45] M. R., *Color physics for Industry*. Society of Dyers and Colorists, Bradford, 1987.

[46] F. R. A. S. T. SMITH, M.A., F.INsT.P., J. GUILD, A.R.C.S., F.INsT.P., "THE C.I.E. COLORIMETRIC STANDARDS AND THEIR USE," *Trans. Opt. Soc.*, vol. XXXIII, no. 3, 1932.

[47] Daniel Malacara, "Color Vision and Colorimetry theory and Applications," 2nd ed., Society of Photo-Optical Instrumentation Engineers (SPIE), 2011.

[48] R. P. C. O. Crick *et al.*, *A TEXTBOOK of CLINICAL OPHTHALMOLOGY*. World Scientific Publishing Co. Pte. Ltd., 2003.

[49] T. Root, *Ophthobook*. CreateSpace Independent Publishing Platform, 2009.

[50] J. Serup and T. Agner, "Colorimetric quantification of erythema-a comparison of two colorimeters (Lange Micro Color and Minolta Chroma Meter CR-200) with a clinical scoring scheme and laser-Doppler flowmetry," *Clin. Exp. Dermatol.*, vol. 15, no. 4, pp. 267–272, Jul. 1990.

[51] C. Queille-Roussel, M. Poncet, and H. Schaefer, "Quantification of skin-colour changes induced by topical corticosteroid preparations using the Minolta Chroma Meter," *Br J Dermatol*, vol. 124, no. 3, pp. 264–270, 1991.

[52] A. Fullerton, T. Fischer, A. Lahti, K. P. Wilhelm, H. Takiwaki, and J. Serup, "Guidelines for measurement of skin colour and erythema. A report from the Standardization Group of the European Society of Contact Dermatitis.," *Contact dermatitis*, vol. 35, no. 1. pp. 1–10, 1996.

[53] E. Van den Kerckhove, F. Staes, M. Flour, K. Stappaerts, and W. Boeckx, "Reproducibility of repeated measurements on healthy skin with Minolta Chromameter CR-300.," *Skin Res. Technol.*, vol. 7, no. 1, pp. 56–9, 2001.

[54] S. Park, C. Huh, Y. Choe, and J. Youn, "Time course of ultraviolet induced skin reactions evaluated by two different reflectance spectrophotometers : DermaSpectrophotometer A and Minolta spectrometer CM-2002," *Photodermatol. Photoimmunol. Photomed.*, vol. 18, pp. 23–28, 2002.

[55] C. K. Kraemer, D. B. Menegon, and T. F. Cestari, "Determination of the minimal phototoxic dose and colorimetry in psoralen plus ultraviolet A radiation therapy," *Photodermatol. Photoimmunol. Photomed.*, vol. 21, no. 5, pp. 242–248, 2005.

[56] M. D. Shriver and E. J. Parra, "Comparison of narrow-band reflectance spectroscopy and tristimulus colorimetry for measurements of skin and hair color in persons of different biological ancestry," *Am. J. Phys. Anthropol.*, vol. 112, no. 1, pp. 17–27, 2000.

[57] L. J. Draaijers, F. R. . Tempelman, Y. A. . Botman, R. W. Kreis, E. Middelkoop, and P. P. . van Zuijlen, "Colour evaluation in scars: tristimulus colorimeter, narrow-band simple reflectance meter or subjective evaluation?," *Burns*, vol. 30, no. 2, pp. 103–107, 2004.

[58] M. Baquie and B. Kasraee, "Discrimination between cutaneous pigmentation and erythema: Comparison of the skin colorimeters Dermacatch and Mexameter," *Ski. Res. Technol.*, vol. 20, no. 2, pp. 218–227, 2014.

[59] A. R. Matias, M. Ferreira, P. Costa, and P. Neto, "Skin colour, skin redness and melanin biometric measurements: Comparison study between Antera-3D, Mexameter and Colorimeter," *Ski. Res. Technol.*, pp. 346–362, 2015.

[60] K. Yoshimura, K. Harii, Y. Masuda, M. Takahashi, T. Aoyama, and T. Iga, "Usefulness of a narrow-band reflectance spectrophotometer in evaluating effects of depigmenting treatment," *Aesthetic Plast. Surg.*, vol. 25, no. 2, pp. 129–133, 2001.

[61] B. L. Diffey, R. J. Oliver, and P. M. Farr, "A portable instrument for quantifying erythema induced by ultraviolet radiation," *Br. J. Dermatol.*, vol. 111, no. 6, pp. 663–672, Dec. 1984.

[62] P. M. Farr and B. L. Diffey, "Quantitative studies on cutaneous erythema induced by ultraviolet radiation.," *Br. J. Dermatol.*, vol. 111, no. 6, pp. 673–682, 1984.

[63] J. R. Trevithick *et al.*, "Topical tocopherol acetate reduces post-UVB, sunburn-associated erythema, edema, and skin sensitivity in hairless mice," *Arch. Biochem. Biophys.*, vol. 296, no. 2, pp. 575–582, 1992.

[64] s poon t c, j m kuchel, A. Badruddin, and G. M. Halliday, "Objective measurement of minimal erythemal and melanogenic doses using natural and solar simulated light," *Photochem. Photobiol.*, vol. 78, no. 4, pp. 331–336, 2003.

[65] E. S. Park, J. I. Na, S. O. Kim, C. H. Huh, S. W. Youn, and K. C. Park, "Application of a pigment measuring device - Mexameter - for the differential diagnosis of vitiligo and nevus depigmentosus," *Ski. Res. Technol.*, vol. 12, no. 4, pp. 298–302, 2006.

[66] K. S. Cheng, M. W. Huang, and P. Y. Lo, "Objective assessment of sunburn and minimal erythema doses: Comparison of noninvasive in vivo measuring techniques after UVB irradiation," *EURASIP J. Adv. Signal Process.*, vol. 2010, pp. 1–7, 2010.

[67] E. J. Yoshida, H. Chen, M. A. Torres, W. J. Curran, and T. Liu, "Spectrophotometer and ultrasound evaluation of late toxicity following breast-cancer radiotherapy.," *Med. Phys.*, vol. 38, no. 10, pp. 5747–55, 2011.

[68] M. Hajizadeh-Saffar, J. W. Feather, and J. B. Dawson, "An investigation of factors affecting the accuracy of in vivo measurements of skin pigments by reflectance spectrophotometry," *Phys. Med. Biol. Phys. Med. Biol*, vol. 35, no. 9, pp. 1301–1315, 1990.

[69] M. S. Patterson, B. Chance, and B. C. Wilson, "Time resolved reflectance and transmittance for the non-invasive measurement of tissue optical properties," *Appl. Opt.*, vol. 28, no. 12, pp. 2331–2336, 1989.

[70] D. T. Delpy, M. Cope, P. van der Zee, S. Arridge, S. Wray, and J. Wyatt, "Estimation of optical pathlength through tissue from direct time of flight measurement.," *Phys. Med. Biol.*, vol. 33, no. 12, pp. 1433–1442, 1988.

[71] M. S. Patterson, J. D. Moulton, B. C. Wilson, K. W. Berndt, and J. R. Lakowicz, "Frequency-domain reflectance for the determination of the scattering and absorption properties of tissue," *Appl. Opt.*, vol. 30, no. 31, pp. 4474–4476, 1991.

[72] M. S. Patterson and B. W. Pogue, "Mathematical model for time-resolved and frequency-domain fluorescence spectroscopy in biological tissues," *Appl. Opt.*, vol. 33, no. 10, pp. 1963–1974, 1994.

[73] N. Kollias, I. Seo, and P. R. Bargo, "Interpreting diffuse reflectance for in vivo skin reactions in terms of chromophores," *J. Biophotonics*, vol. 3, no. 1–2, pp. 15–24, 2010.

[74] L. Lim, B. Nichols, N. Rajaram, and J. W. Tunnell, "Probe pressure effects on human skin diffuse reflectance and fluorescence spectroscopy measurements," *J. Biomed. Opt.*, vol. 16, no. 1, p. 11012, 2011.

[75] J. R. Mallia, S. S. Thomas, and P. Sebastian, "Oral cancer detection using diffuse reflectance spectral ratio R540 / R575 of oxygenated hemoglobin bands," vol. 11, no. February 2006, pp. 1–6, 2017.

[76] A. H. Taylor, "The measurement of diffuse reflection factors and a new absolute reflectometer," *J. Opt. Soc. Am.*, vol. 4, no. 1–2, p. 9, 1920.

[77] J. a. Jacquez and H. F. Kuppenheim, "Theory of the Integrating Sphere," *J. Opt. Soc. Am.*, vol. 45, no. 6, p. 460, 1955.

[78] J. W. Pickering, C. J. M. Moes, H. J. C. M. Sterenborg, S. A. Prahl, and M. J. C. van Gemert, "Two integrating spheres with an intervening scattering sample," *J. Opt. Soc. Am. A*, vol. 9, no. 4, pp. 621–631, 1992.

[79] J. W. Pickering, S. a Prahl, N. van Wieringen, J. F. Beek, H. J. Sterenborg, and M. J. van Gemert, "Double-integrating-sphere system for measuring the optical properties of tissue.," *Appl. Opt.*, vol. 32, no. 4, pp. 399–410, 1993.

[80] T. J. Farrell, "A diffusion theory model of spatially resolved, steady-state diffuse reflectance for the noninvasive determination of tissue optical properties in vivo," *Med. Phys.*, vol. 19, no. 4, p. 879, 1992.

[81] a Kienle, L. Lilge, M. S. Patterson, R. Hibst, R. Steiner, and B. C. Wilson, "Spatially resolved absolute diffuse reflectance measurements for noninvasive determination of the optical scattering and absorption coefficients of biological tissue.," *Appl. Opt.*, vol. 35, no. 13, pp. 2304–2314, 1996.

[82] R. M. Doornbos, R. Lang, M. C. Aalders, F. W. Cross, and H. J. Sterenborg, "The determination of in vivo human tissue optical properties and absolute chromophore concentrations using spatially resolved steady-state diffuse reflectance spectroscopy.," *Phys. Med. Biol.*, vol. 44, no. 4, pp. 967–981, 1999.

[83] A. Pifferi *et al.*, "Spectroscopic time-resolved diffuse reflectance and transmittance measurements of the female breast at different interfiber distances.," *J. Biomed. Opt.*, vol. 9, no. 6, pp. 1143–51, 2004.

[84] D. F. Moscu, "Quantifying chromophore concentration in tissue simulating phantoms using an optical detection system based on an integrating sphere," p. 153, 2010.

[85] D. F. Moscu, "Quantifying chromophore concentration in tissue simulating phantoms using an optical

detection system based on an integrating sphere," 2010.

[86] K. Wårdell, H. K. Naver, G. E. Nilsson, and B. G. Wallin, "The cutaneous vascular axon reflex in humans characterized by laser Doppler perfusion imaging.," *J. Physiol.*, vol. 460, pp. 185–199, 1993.

[87] G. Heyer, O. P. Hornstein, and H. O. Handwerker, "Skin reactions and itch sensation induced by epicutaneous histamine application in atopic dermatitis and controls," *J Invest Dermatol*, vol. 93, no. 4, pp. 492–496, 1989.

[88] G. V Oliveira, D. Chinkes, C. Mitchell, G. Oliveras, H. K. Hawkins, and D. N. Herndon, "Objective assessment of burn scar vascularity, erythema, pliability, thickness, and planimetry.," *Dermatol. Surg.*, vol. 31, pp. 48–58, 2005.

[89] S. B. Phillips, N. Kollias, R. Gillies, J. A. Muccini, and L. A. Drake, "Polarized light photography enhances visualization of inflammatory lesions of acne vulgaris," *J. Am. Acad. Dermatol.*, vol. 37, no. 6, pp. 948–952, 1997.

[90] A. C. Halpern, A. A. Marghoob, T. W. Bialoglow, W. Witmer, and W. Slue, "Standardized positioning of patients (poses) for whole body cutaneous photography," *J. Am. Acad. Dermatol.*, vol. 49, no. 4, pp. 593–598, 2003.

[91] W. K. Witmer and P. J. Lebovitz, "Clinical Photography in the Dermatology Practice," *Semin. Cutan. Med. Surg.*, vol. 31, no. 3, pp. 191–199, 2012.

[92] A. Raina, R. Hennessy, M. Rains, J. Allred, D. Diven, and M. K. Markey, "Objective measurement of erythema in psoriasis using digital color photography with color calibration," *Ski. Res. Technol.*, no. 7, pp. 1–6, 2015.

[93] M. Setaro and A. Sparavigna, "Quantification of erythema using digital camera and computer-based colour image analysis: a multicentre study.," *Skin Res. Technol.*, vol. 8, no. 2, pp. 84–8, 2002.

[94] D. Hossam, A. Sadek, A. Wagih, and M. Malik, "Clinical photography of skin diseases," *Egypt. Dermatology Online J.*, vol. 11, no. 1, pp. 1–10, 2015.

[95] "CANFIELD." [Online]. Available: http://www.canfieldsci.com/imaging-systems/visia-cr/.

[96] S. G. Coelho, S. A. Miller, B. Z. Zmudzka, and J. Z. Beer, "Quantification of UV-Induced Erythema and Pigmentation Using Computer-Assisted Digital Image Evaluation," *Photochem. Photobiol.*, vol. 82, no. 3, pp. 651–655, 2006.

[97] S. Taylor, W. Westerhof, S. Im, and J. Lim, "Noninvasive techniques for the evaluation of skin color," *J. Am. Acad. Dermatol.*, vol. 54, no. 5, pp. S282–S290, 2006.

[98] A. K. CC Zouboulis, AD Katsambas, *Pathogenesis and Treatment of Acne and Rosacea*. Springer-Verlag Berlin Heidelberg, 2014.

[99] S. Sridhar and A. Da Silva, "Enhanced contrast and depth resolution in polarization imaging using elliptically polarized light," *J. Biomed. Opt.*, vol. 21, no. 7, p. 71107, 2016.

[100] Z. Huang *et al.*, "Cutaneous melanin exhibiting fluorescence emission under near-infrared light excitation.," *J. Biomed. Opt.*, vol. 11, no. 3, p. 34010, 2006.

[101] J. O'doherty, J. Henricson, C. Anderson, M. J. Leahy, G. E. Nilsson, and F. Sjoberg, "Sub-epidermal imaging using polarized light spectroscopy for assessment of skin microcirculation," *Ski. Res. Technol.*, vol. 13, no. 4, pp. 472–484, 2007.

[102] J. M. Gallas and M. Eisner, "Fluorescence of Melanin-Dependence Upon Excitation Wavelength and Concentration," *Photochem. Photobiol.*, vol. 45, no. 5, pp. 595–600, 1987.

[103] N. Kollias *et al.*, "Fluorescence photography in the evaluation of hyperpigmentation in photodamaged skin," *J. Am. Acad. Dermatol.*, vol. 36, no. 2, pp. 226–300, 1997.

[104] R. J. T. Leslie C. Lucchina, Scott B. Phillips, "Fluorescence photography in the evaluation of acne," *Am. Acad. Dermatology*, 1996.

[105] A. Tosti *et al.*, "Follicular Red Dots," *Arch Dermatol*, vol. 145, no. 12, pp. 1406–1409, 2009.

[106] A. N. Yaroslavsky, J. Barbosa, V. Neel, C. DiMarzio, and R. R. Anderson, "Combining multispectral polarized light imaging and confocal microscopy for localization of nonmelanoma skin cancer.," *J. Biomed. Opt.*, vol. 10, no. 1, p. 14011, 2005.

[107] M. Rajadhyaksha, S. González, J. M. Zavislan, R. R. Anderson, and R. H. Webb, "In vivo confocal scanning laser microscopy of human skin II: advances in instrumentation and comparison with histology.," *J. Invest. Dermatol.*, vol. 113, no. 3, pp. 293–303, 1999.

[108] S. Astner, E. Gonzalez, A. Cheung, F. Rius-Diaz, and S. González, "Pilot study on the sensitivity and specificity of in vivo reflectance confocal microscopy in the diagnosis of allergic contact dermatitis," *J. Am. Acad. Dermatol.*, vol. 53, no. 6, pp. 986–992, 2005.

[109] S. Astner, N. Burnett, F. Rius-Díaz, A. G. Doukas, S. González, and E. Gonzalez, "Irritant contact dermatitis induced by a common household irritant: A noninvasive evaluation of ethnic variability in skin response," *J. Am. Acad. Dermatol.*, vol. 54, no. 3, pp. 458–465, 2006.

[110] J. a Suárez-Pérez, "Pathogenesis and diagnosis of contact dermatitis: Applications of reflectance confocal microscopy," *World J. Dermatology*, vol. 3, no. 3, p. 45, 2014.

[111] R. Proc *et al.*, "Imaging Spectroscopy Using Tunable Filters: A Review," Apr. 2000.

[112] D. a Glenar, J. J. Hillman, B. Saif, and J. Bergstralh, "Acousto-optic imaging spectropolarimetry for remote sensing.," *Appl. Opt.*, vol. 33, no. 31, pp. 7412–24, Nov. 1994.

[113] L. Kong *et al.*, "Handheld erythema and bruise detector," *Proc. SPIE*, vol. 6915, p. 69153K–69153K–7, 2008.

[114] D. Jakovels, J. Spigulis, and I. Saknite, "Multi-spectral mapping of in vivo skin hemoglobin and melanin," *SPIE Proc.*, vol. 7715, p. 77152Z--77152Z, 2010.

[115] J. M. Beach, M. a. Lanoue, K. Brabham, and B. Khoobehi, "Portable hyperspectral imager for assessment of skin disorders: preliminary measurements," in *Photonic Therapeutics and Diagnostics, Proc. of SPIE*, 2005, vol. 5686, pp. 111–118.

[116] Z. Nie, R. An, J. E. Hayward, T. J. Farrell, and Q. Fang, "Hyperspectral fluorescence lifetime imaging for optical biopsy.," *J. Biomed. Opt.*, vol. 18, no. 9, p. 96001, Sep. 2013.

[117] C. Zhang and H. Wang, "The narrow band AOTF based hyperspectral microscopic imaging on the rat skin stratum configuration," *J.Europ.Opt.Soc.*, vol. 14034, 2014.

[118] a. D. Meigs, I. Otten, L.J., and T. Y. Cherezova, "Ultraspectral imaging: a new contribution to global virtual presence," in *1998 IEEE Aerospace Conference Proceedings (Cat. No.98TH8339)*, 1998, vol. 2, no. October.

[119] A. F. H. Goetz, "Three decades of hyperspectral

remote sensing of the Earth: A personal view," *Remote Sens. Environ.*, vol. 113, pp. S5–S16, 2009.
[120] G. Lu and B. Fei, "Medical hyperspectral imaging: a review.," *J. Biomed. Opt.*, vol. 19, no. 1, p. 10901, Jan. 2014.
[121] N. Kollias, R. Gillies, J. A. Muccini, R. K. Uyeyama, S. B. Phillips, and L. A. Drake, "A Single Parameter, Oxygenated Hemoglobin, Can Be Used to Quantify Experimental Irritant-Induced Inflammation," *J. Invest. Dermatol.*, vol. 104, no. 3, pp. 421–424, 1995.
[122] G. N. Stamatas, C. J. Balas, and N. Kollias, "Hyperspectral Image Acquisition and Analysis of Skin," in *Spectral Imaging: Instrumentation, Applications, and Analysis II, Proceedings of SPIE*, 2003, vol. 4959, pp. 77–82.
[123] G. N. Stamatas, M. Southall, and N. Kollias, "In vivo monitoring of cutaneous edema using spectral imaging in the visible and near infrared.," *J. Invest. Dermatol.*, vol. 126, no. 8, pp. 1753–1760, 2006.
[124] G. N. Stamatas and N. Kollias, "In vivo documentation of cutaneous inflammation using spectral imaging.," *J. Biomed. Opt.*, vol. 12, no. 5, p. 51603, 2007.
[125] M. S. Chin *et al.*, "Hyperspectral imaging for early detection of oxygenation and perfusion changes in irradiated skin," *J. Biomed. Opt.*, vol. 17, no. 2, p. 26010, 2012.
[126] G. V. G. Baranoski, S. Member, T. F. Chen, and S. Member, "On the Identification and Interpretation of Human Skin Spectral Responses Under Adverse Environmental Conditions," pp. 845–848, 2015.
[127] G. N. Stamatas and N. Kollias, "In vivo documentation of cutaneous inflammation using spectral imaging.," *J. Biomed. Opt.*, vol. 12, no. 5, p. 51603, 2007.
[128] S. Zhang, P. Liu, J. Huang, and R. Xu, "Multiview hyperspectral topography of tissue structural and functional characteristics," *J. Biomed. Opt.*, vol. 21, p. 85530P–85530P–7, 2016.
[129] S. Zhang, P. Liu, J. Huang, and R. Xu, "Multiview hyperspectral topography of tissue structural and functional characteristics," *J. Biomed. Opt.*, vol. 21, p. 85530P–85530P–7, 2016.
[130] J. Nyström, P. Geladi, B. Lindholm-Sethson, J. Rattfelt, A. C. Svensk, and L. Franzen, "Objective measurements of radiotherapy-induced erythema," *Ski. Res. Technol.*, vol. 10, no. 4, pp. 242–250, 2004.
[131] J. O'doherty, J. Henricson, C. Anderson, M. J. Leahy, G. E. Nilsson, and F. Sj??berg, "Sub-epidermal imaging using polarized light spectroscopy for assessment of skin microcirculation," *Ski. Res. Technol.*, vol. 13, no. 4, pp. 472–484, 2007.
[132] A. K. CC Zouboulis, AD Katsambas, *Pathogenesis and Treatment of Acne and Rosacea*. Springer-Verlag Berlin Heidelberg, 2014.
[133] M. Boone, G. B. E. Jemec, and V. Del Marmol, "High-definition optical coherence tomography enables visualization of individual cells in healthy skin: Comparison to reflectance confocal microscopy," *Exp. Dermatol.*, vol. 21, no. 10, pp. 740–744, 2012.
[134] T. Gambichler, G. Moussa, M. Sand, D. Sand, P. Altmeyer, and K. Hoffmann, "Applications of optical coherence tomography in dermatology," *J. Dermatol. Sci.*, vol. 40, no. 2, pp. 85–94, 2005.
[135] J. W. Elke Sattler, Raphaela Kastle, "Optical coherence tomography in dermatology," *J. Biomed. Opt.*, vol. 18, no. 6, 2013.
[136] D. L. M. Harold Alexander, "Determining Skin Thickness with Pulsed Ultra Sound," *J. Invest. Dermatol.*, vol. 72, no. 1, pp. 17–19, 1979.
[137] A. Warszawski, E. M. Röttinger, R. Vogel, and N. Warszawski, "20 MHz ultrasonic imaging for quantitative assessment and documentation of early and late postradiation skin reactions in breast cancer patients," *Radiother. Oncol.*, vol. 47, no. 3, pp. 241–247, 1998.
[138] E. Szymańska *et al.*, "Skin imaging with high frequency ultrasound - preliminary results.," *Eur. J. Ultrasound*, vol. 12, pp. 9–16, 2000.
[139] X. Wortsman and J. Wortsman, "Clinical usefulness of variable-frequency ultrasound in localized lesions of the skin," *J. Am. Acad. Dermatol.*, vol. 62, no. 2, pp. 247–256, 2010.
[140] S. Wong, A. Kaur, M. Back, K. M. Lee, S. Baggarley, and J. J. Lu, "An ultrasonographic evaluation of skin thickness in breast cancer patients after postmastectomy radiation therapy.," *Radiat. Oncol.*, vol. 6, no. 1, p. 9, 2011.
[141] X. Wortsman, J. Wortsman, C. Orlandi, G. Cardenas, I. Sazunic, and G. B. E. Jemec, "Ultrasound detection and identification of cosmetic fillers in the skin," *J. Eur. Acad. Dermatology Venereol.*, vol. 26, no. 3, pp. 292–301, 2012.
[142] R. Kleinerman, T. B. Whang, R. L. Bard, and E. S. Marmur, "Ultrasound in dermatology: Principles and applications," *J. Am. Acad. Dermatol.*, vol. 67, no. 3, pp. 478–487, 2012.
[143] X. Wortsman and J. Wortsman, "Clinical usefulness of variable-frequency ultrasound in localized lesions of the skin," *J. Am. Acad. Dermatol.*, vol. 62, no. 2, pp. 247–256, 2010.
[144] a B. Kimball *et al.*, "Magnetic resonance imaging detection of occult skin and subcutaneous abnormalities in juvenile dermatomyositis. Implications for diagnosis and therapy.," *Arthritis Rheum.*, vol. 43, no. 8, pp. 1866–73, 2000.
[145] B. Querleux, "Magnetic resonance imaging and spectroscopy of skin and subcutis," *J Cosmet Dermatol*, vol. 3, no. 3, pp. 156–161, 2004.
[146] E. Burdette, F. Cain, and J. Seals, "In vivo probe measurement technique for determining dielectric properties at VHF through microwave frequencies," *IEEE Trans. Microw. Theory Tech.*, vol. MTT-28, no. 4, pp. 414–427, 1980.
[147] J. Nuutinen *et al.*, "A dielectric method for measuring early and late reactions in irradiated human skin," *Radiother. Oncol.*, vol. 47, no. 3, pp. 249–254, 1998.
[148] B. Riordan, S. Sprigle, and M. Linden, "Testing the validity of erythema detection algorithms.," *J. Rehabil. Res. Dev.*, vol. 38, no. 1, pp. 13–22, 2001.
[149] I. Diebele, A. Bekina, A. Derjabo, J. Kapostinsh, I. Kuzmina, and J. Spigulis, "Analysis of skin basalioma and melanoma by multispectral imaging," *Biophotonics*, vol. 8427, no. May, pp. 842732-842732–5, 2012.
[150] H. Tronnier, "Evaluation and measurement of ultraviolet erythema," *Biol. Eff. Ultrav. Radiat.*, pp. 255–266, 1969.
[151] B. L. Diffey and P. M. Farr, "Quantitative aspects of ultraviolet erythema," *Clin. Phys. Physiol. Meas.*, vol. 12, no. 4, p. 311, 1991.
[152] M. Ferguson-Pell and S. Hagisawa, "An empirical technique to compensate for melanin when monitoring skin microcirculation using reflectance spectrophotometry," *Med. Eng. Phys.*, vol. 17, no. 2, pp. 104–110, 1995.
[153] J. W. Feather, M. Hajizadeh-Saffar, G. Leslie, and J. B. Dawson, "A portable scanning reflectance spectrophotometer using visible wavelengths for the rapid measurement of skin pigments.," *Phys. Med.*

Biol., vol. 34, no. 7, pp. 807–820, 1989.
[154] J. B. Dawson *et al.*, "A theoretical and experimental study of light absorption and scattering by in vivo skin.," *Phys. Med. Biol.*, vol. 25, no. 4, pp. 695–709, 1980.
[155] E. Held, H. Lorentzen, T. Agner, and T. Menné, "Comparison between visual score and erythema index (DermaSpectrometer) in evaluation of allergic patch tests," *Ski. Res. Technol.*, vol. 4, no. 4, pp. 188–191, 1998.
[156] D. M. Cockburn, "Confessions of a colour blind optometrist," *Clin. Exp. Optom.*, vol. 87, no. 4–5, pp. 350–352, 2004.
[157] P. R. Bargo *et al.*, "In vivo determination of optical properties of normal and tumor tissue with white light reflectance and an empirical light transport model during endoscopy.," *J. Biomed. Opt.*, vol. 10, no. 3, p. 34018, 2005.